

TECHNICAL REPORT 94-13

**KRISTALLIN-I:
Repository Layout Study
Preliminary Calculation of
Temperature Distributions
around an Emplacement Tunnel**

September 1998

Obayashi Corporation

TECHNICAL REPORT 94-13

KRISTALLIN-I: Repository Layout Study Preliminary Calculation of Temperature Distributions around an Emplacement Tunnel

September 1998

Obayashi Corporation

This report was prepared on behalf of Nagra. The viewpoints presented and conclusions reached are those of the author(s) and do not necessarily represent those of Nagra.

ISSN 1015-2636

"Copyright © 1998 by Nagra, Wettingen (Switzerland) / All rights reserved.

All parts of this work are protected by copyright. Any utilisation outwith the remit of the copyright law is unlawful and liable to prosecution. This applies in particular to translations, storage and processing in electronic systems and programs, microfilms, reproductions, etc."

Summary

The main aim of this study is to derive an understanding of the effect of tunnel spacing on temperature distributions around a HLW emplacement tunnel (diameter 3.7 m), located in the crystalline basement of Northern Switzerland. In Project Gewähr 1985, the tunnel spacing was tentatively set at 40 m, assuming that the extent of an undisturbed rock block was sufficiently large to accommodate a regular-shaped reference repository concept. The detailed geological investigations that were synthesized in the Kristallin-I Project provided preliminary indications of the size of undisturbed blocks that would be expected. Although indicating that there is a good chance of finding one or more suitable blocks, the actual block dimensions will not be known until the results of more detailed exploration are available. The chance of finding suitable blocks is, however, higher if the repository is designed with a compact layout. This provides the motivation for the studies on the extent to which the tunnel spacing can be reduced without compromising safety. Safety might be compromised either through loss of tunnel stability or through excessive temperatures arising in the near-field (and, particularly significantly, in the bentonite) due to radiogenic heat from the HLW. In the present study, tunnel spacing is varied to investigate its effect on the maximum temperature in the bentonite. Furthermore, the bentonite thermal properties and the presence of air gaps are also treated as variable parameters.

An important conclusion of this study is the recommendation that the horizontal spacing of emplacement tunnels should not be less than around 20 m, to ensure that tunnel spacing has little influence on temperature profiles. Modeled temperatures of all the near-field components tend to increase significantly if tunnel spacing is less than around 20 m. It should be noted that this conclusion is provisional, being based on idealized numerical calculations and model parameters. However, the authors feel that this represents valuable input for preliminary HLW repository design studies.

No significant temperature differences are observed between cases where the thermal properties of the bentonite are a function of variable water content ($\phi = 7 - 0\%$, Analyses No. 1 to 3) and those where water content is kept constant ($\phi = 2\%$, Analyses No. 4 to 6). Thus, it is concluded that temperature distributions in the near-field are insensitive to bentonite thermal properties. As further examples, Analyses No. 10 to 12 are performed with less conservative bentonite thermal properties. It is assumed that no air gaps exist in the bentonite and the tunnel spacing is kept at 20 m. It is then found that temperature profiles are sensitive to the thermal conductivity of the bentonite but insensitive to its thermal capacity.

Finally, it is worth noting that the feasibility of ensuring the absence of air gaps in the bentonite is uncertain and should be investigated because temperature distributions are sensitive to the presence of such gaps.

Zusammenfassung

Die vorliegende Studie hat die Abklärung der Auswirkungen des Stollenabstands auf die Temperaturverteilung um einen HAA Einlagerungsstollen (Durchmesser 3.7 m) im kristallinen Grundgebirge der Nordschweiz zum Hauptziel. Im Projekt Gewähr 1985 wurde der Stollenabstand vorläufig auf 40 m festgelegt, unter der Annahme, dass die Ausdehnung eines ungestörten Gesteinsblocks genügend gross für ein Referenzkonzept mit regelmässiger Endlagergeometrie ist. Die im Projekt Kristallin-I dokumentierten eingehenden geologischen Untersuchungen lieferten erste Hinweise über die Grösse der erwarteten ungestörten Blöcke. Obwohl es Hinweise dafür gibt, dass gute Chancen bestehen, einen oder mehrere geeignete Blöcke aufzufinden, werden die tatsächlichen Blockabmessungen erst nach detaillierteren Untersuchungen bekannt sein. Ein kompaktes Endlagerlayout erhöht jedoch die Wahrscheinlichkeit, solche geeigneten Blöcke aufzufinden. Daher wurde die vorliegende Studie veranlasst, um abzuklären, inwieweit der Stollenabstand verringert werden kann ohne die Sicherheit der Endlagerung zu beeinträchtigen. Eine Beeinträchtigung der Sicherheit könnte entweder durch Verlust der Stollenstabilität oder übermässig hohe Temperaturen im Nahfeld (insbesondere im Bentonit) durch die Zerfallswärme der HAA verursacht werden. In der vorliegenden Studie wird der Stollenabstand variiert, um dessen Auswirkungen auf die Maximaltemperaturen im Bentonit zu untersuchen. Die thermischen Eigenschaften des Bentonits und die Präsenz von luftdurchlässigen Spalten im Bentonit werden auch als variable Parameter behandelt.

Eine wichtige Schlussfolgerung dieser Studie ist die Empfehlung, dass der horizontale Abstand von Einlagerungsstollen nicht kleiner als ca. 20 m betragen soll, um zu gewährleisten, dass dieser Parameter einen vernachlässigbaren Einfluss auf die Temperaturprofile ausübt. Die modellierten Temperaturen aller Nahfeld-Komponenten steigen bedeutend an, wenn der Stollenabstand kleiner als ca. 20 m ist. Es sollte klar betont werden, dass diese Schlussfolgerung nur provisorisch ist, da sie auf idealisierten numerischen Berechnungen und Modellparametern basiert. Nach Ansicht der Autoren liefern sie jedoch einen wertvollen Input für erste HAA Endlagerdesignstudien.

In Fällen, in denen die thermischen Eigenschaften des Bentonits eine Funktion des variablen Wassergehalts sind ($\phi = 7 - 0\%$, Analysen Nr. 1 bis 3) wurden gegenüber solchen mit konstant gehaltenem Wassergehalt ($\phi = 2\%$, Analysen Nr. 4 bis 6) keine bedeutenden Temperaturunterschiede beobachtet. Daraus kann geschlossen werden, dass die Temperaturverteilung im Nahfeld nicht sensitiv ist auf die thermischen Eigenschaften des Bentonits. Als weitere Beispiele können die Analysen Nr. 10 bis 12 angeführt werden, die mit weniger konservativen thermischen Eigenschaften des Bentonits durchgeführt wurden. In diesem Fall kann festgestellt werden, dass die Temperaturprofile sensitiv auf die Wärmeleitfähigkeit des Bentonits reagieren, aber nicht auf dessen Wärmekapazität.

Schliesslich soll bemerkt werden, dass die Realisierbarkeit einer Bentonitverfüllung, bei der gewährleistet werden kann, dass keine luftdurchlässigen Spalten im Bentonit vorhanden sind, ungewiss ist. Dies sollte weiter untersucht werden, da die Temperaturverteilungen auf die Anwesenheit solcher Spalten sensitiv sind.

Exposé de synthèse

L'objectif principal de cette étude est de développer une compréhension de l'impact du facteur « espacement » des galeries de stockage sur la distribution des températures autour d'un tunnel de desserte (diamètre 3.7 m) d'un stockage de déchets radioactifs à haute activité, supposé situé dans le socle cristallin du nord de la Suisse. Dans le cadre du Projet « Gewähr » de 1985, l'espacement des galeries a été défini provisoirement à 40 m, sous l'hypothèse de l'existence d'un bloc de roche non perturbée et de dimensions suffisantes pour y insérer un stockage de référence de forme régulière. Les investigations géologiques détaillées du projet Cristallin-I ont fourni les premières indications sur la dimension des blocs de roche non-perturbés que l'on pouvait attendre. Bien qu'il y ait une bonne chance de trouver un ou plusieurs blocs adéquats, les vraies dimensions de tels blocs ne seront pas connues avant que l'on réalise une exploration plus détaillée. Les chances de trouver des blocs de dimension adéquate sont toutefois plus fortes si le stockage est conçu de manière compacte. Ceci a motivé l'étude des dimensions auxquelles le stockage pouvait être réduit sans compromettre sa sûreté. La sûreté peut être compromise soit par une perte de stabilité des galeries, soit par des températures excessives dans le champ proche des déchets, et particulièrement dans la bentonite, provoquées par la chaleur dégagée par les déchets de haute activité. Dans la présente étude, on fait varier l'espacement entre les galeries pour étudier son effet sur les températures maximales dans la bentonite. De plus, les propriétés thermiques de la bentonite et la présence de vides interstitiels remplis d'air sont aussi traitées comme des variables de dimensionnement.

Une conclusion importante de cette étude est que l'espacement horizontal entre les galeries ne devrait pas être inférieur à 20 m environ, pour qu'il n'ait que peu d'influence sur les profils de température. Les températures simulées de tous les éléments du champ proche ont tendance à croître de manière significative si l'espacement entre les galeries est inférieur à 20 m. Ces résultats doivent être considérés comme provisoires, car basés sur des hypothèses, paramètres et modèles numériques simplificateurs. Toutefois, ces résultats fournissent des données d'entrée pour les études de conception préliminaires sur le stockage de déchets radioactifs de haute activité.

Il n'a pas été observé de différence significative de température entre les cas où les propriétés thermiques de la bentonite sont fonction d'une teneur en eau variable ($\phi = 7 - 0 \%$, analyses n° 1 à 3) et les cas où la teneur en eau est gardée constante ($\phi = 2\%$, analyses n° 4 à 6). Ainsi, on en conclut que la distribution des températures dans le champ proche est insensible aux propriétés thermiques de la bentonite. D'autres analyses (n° 10 à 12) ont été conduites avec des propriétés thermiques de la bentonite plus favorables : Il a été admis qu'il n'y avait pas de vides interstitiels remplis d'air dans la bentonite et l'espacement des galeries a été maintenu à 20 m. Les profils de température sont alors sensibles à la conductivité thermique de la bentonite, mais pas à sa capacité thermique.

Enfin, il faut mentionner qu'il est n'est pas certain que l'on puisse assurer une absence totale d'air interstitiel dans la bentonite. La faisabilité d'une bentonite sans air interstitiel devrait être étudiée, car la distribution des températures y est sensible.

Table of Contents

Summary	I
Zusammenfassung.....	II
Exposé de synthèse	III
Table of Contents	IV
List of Tables.....	V
List of Figures	V
1 Introduction	1
2 Modeling and thermal properties.....	2
2.1 Analysis and models.....	2
2.2 Geometric modeling and temperature conditions.....	2
2.2.1 Canister.....	2
2.2.2 Emplacement tunnels.....	4
2.2.3 Depth, initial temperatures and analysis domain.....	4
2.2.4 Air gaps in the bentonite.....	5
2.3 Heat production	6
2.4 Thermal properties of system components.....	7
2.4.1 Bentonite.....	7
2.4.2 Other components.....	10
2.5 Schematic representation of the model and boundary conditions	11
2.6 Variable parameters selected for the numerical analyses in this study.....	14
3 Calculated temperature distributions	15
3.1 Maximum temperatures of each component.....	15
3.2 Temperature profiles and temperature-time histories.....	17
3.3 Comparison with the temperature outputs for Project Gewähr 1985	32
3.4 Effect of tunnel spacing on temperature distributions.....	32
3.5 Effect of bentonite thermal properties on temperature distributions	35
3.6 Effect of air gaps on temperature distributions.....	37
4 Summary and conclusions	40
5 References.....	41

List of Tables

Tab. 2-1:	Heat production values for vitrified waste used in this study (ALDER & MCGINNES 1993)	6
Tab. 2-2:	Thermal properties of bentonite blocks	8
Tab. 2-3:	Cross-comparison of bentonite thermal properties.....	8
Tab. 2-4:	Thermal properties of bentonite for this study.....	10
Tab. 2-5:	Thermal properties of the other components for this study	11
Tab. 2-6:	Parameters selected for the numerical analyses in this study	14
Tab. 3-1:	Maximum temperatures [°C] in various components and their time of occurrence after emplacement	16

List of Figures

Fig. 2-1:	Geometry of the Nagra reference cast steel canister (dimensions in mm; NAGRA 1985a)	3
Fig. 2-2:	Canister model used for numerical analyses in this study (dimensions in mm)	3
Fig. 2-3:	Geometry of a horizontal plane through the near-field for the thermal analyses in this study (originally from NAGRA 1985a)	4
Fig. 2-4:	Analysis domain for the thermal analyses in this study (originally from NAGRA 1985a)	5
Fig. 2-5:	Locations of the three air gaps assumed in Project Gewähr 1985 (originally from NAGRA 1985a)	6
Fig. 2-6:	Heat release rate from a high-level reprocessing waste package versus time since unloading of the fuel from the reactor (HOPKIRK & WAGNER 1986)	7
Fig. 2-7:	Water content of bentonite as a function of temperature (HOPKIRK & WAGNER 1986)	9
Fig. 2-8:	Three-dimensional model representation and boundary conditions	12
Fig. 2-9:	Model geometry of the near-field around a tunnel (dimensions in mm)	12
Fig. 2-10:	Example of the three-dimensional finite-element mesh used in this study	13
Fig. 3-1:	Relationship between horizontal tunnel spacing and maximum temperature of bentonite	17
Fig. 3-2:	Temperatures for Analysis No. 1 at 1, 10, 40 and 100 years after emplacement	18
Fig. 3-3:	Location of the temperature output points A to M (dimensions in mm)	19
Fig. 3-4:	Temperature profiles and temperature-time histories of Analysis No. 1	20
Fig. 3-5:	Temperature profiles and temperature-time histories of Analysis No. 2	21
Fig. 3-6:	Temperature profiles and temperature-time histories of Analysis No. 3	22

Fig. 3-7:	Temperature profiles and temperature-time histories of Analysis No. 4.....	23
Fig. 3-8:	Temperature profiles and temperature-time histories of Analysis No. 5.....	24
Fig. 3-9:	Temperature profiles and temperature-time histories of Analysis No. 6.....	25
Fig. 3-10:	Temperature profiles and temperature-time histories of Analysis No. 7.....	26
Fig. 3-11:	Temperature profiles and temperature-time histories of Analysis No. 8.....	27
Fig. 3-12:	Temperature profiles and temperature-time histories of Analysis No. 9.....	28
Fig. 3-13:	Temperature profiles and temperature-time histories of Analysis No. 10.....	29
Fig. 3-14:	Temperature profiles and temperature-time histories of Analysis No. 11.....	30
Fig. 3-15:	Temperature profiles and temperature-time histories of Analysis No. 12.....	31
Fig. 3-16:	Cross-comparison of the temperature profiles calculated in this study with those in Project Gewähr 1985.....	32
Fig. 3-17:	Comparison of temperature profiles and temperature-time histories of Analyses No. 1, 2 and 3 (air gap)	33
Fig. 3-18:	Comparison of temperature profiles and temperature-time histories of Analyses No. 7, 8 and 9 (no air gap)	34
Fig. 3-19:	Temperature profiles of Analyses No. 1 and 4 (tunnel spacing $S_h = 40$ m).....	35
Fig. 3-20:	Temperature profiles of Analyses No. 2 and 5 (tunnel spacing $S_h = 20$ m).....	36
Fig. 3-21:	Temperature profiles of Analyses No. 3 and 6 (tunnel spacing $S_h = 10$ m).....	36
Fig. 3-22:	Temperature profiles of Analyses No. 10, 11 and 12 (tunnel spacing $S_h = 20$ m).....	37
Fig. 3-23:	Temperature profiles of Analyses No. 1 and 7 (tunnel spacing $S_h = 40$ m).....	38
Fig. 3-24:	Temperature profiles of Analyses No. 2 and 8 (tunnel spacing $S_h = 20$ m).....	38
Fig. 3-25:	Temperature profiles of Analyses No. 3 and 9 (tunnel spacing $S_h = 10$ m).....	39

1 Introduction

A series of Nagra/Obayashi collaborative engineering studies for the Kristallin-I Project, termed "KRISTALLIN-I: Repository Layout Study", was carried out as a joint Nagra-Obayashi project and consists of the following three specific tasks.

- 1) Numerical investigation of emplacement tunnel spacing
- 2) Numerical and engineering investigation of tunnel stability in a fracture zone
- 3) Preliminary calculation of temperature distributions around an emplacement tunnel

This report focuses on the third task, namely performing and discussing high-level waste (HLW) near-field temperature calculations. The objective of this study is to evaluate temperature distributions around an emplacement tunnel of a HLW repository located in the crystalline basement of Northern Switzerland in order to optimize emplacement tunnel layout. Temperature is a parameter affecting many processes occurring within the engineered barrier system. Radiogenic heat may generate high temperatures in the waste itself, in the canister containing the waste and in the surrounding backfill material. It is desirable to show that a significant thickness of bentonite does not experience high temperatures (in excess of 100 °C, say) when bentonite is used as a backfill material in order to ensure that its favorable radionuclide retention properties are maintained.

In Project Gewähr 1985 (NAGRA 1985a), the emplacement tunnel spacing, which is one of the key layout elements, was tentatively set at 40 m. In the reference case, it was assumed that the extent of undisturbed crystalline rock would be large enough to accommodate a regular-shaped repository in one block. The detailed geological data on the crystalline basement synthesized in the Kristallin-I Project provided preliminary indications of the size of undisturbed blocks that would be expected. Although indicating that there is a good chance of finding one or more suitable blocks, the actual block dimensions will not be known until the results of more detailed exploration are available. The chance of finding suitable blocks is, however, higher if the repository is designed with a compact layout. This provides the motivation for the studies on the extent to which the tunnel spacing can be reduced without compromising safety. Safety might be compromised either through loss of tunnel stability or through excessive temperatures arising in the near-field (and, particularly significantly, in the bentonite) due to radiogenic heat from the HLW.

In this study, tunnel spacing was varied to investigate its effect on the maximum temperatures of engineered barrier system (EBS) components, especially on that of bentonite. Furthermore, the thermal properties of bentonite and the existence of air gaps were also treated as variable parameters.

Finally, it should be noted that the output from this study is intended to support the revised repository layout by providing constraints or design guidelines. It is considered that the tunnel layout proposed in this study is not optimized but represents an example of a layout that is consistent, in terms of temperature evolution, with long-term repository safety.

2 Modeling and thermal properties

This chapter describes the modeling approach and thermal properties of each component of the near-field used to calculate temperature distributions around and within an emplacement tunnel. The modeling assumptions and thermal properties used in this study were based on the waste management concept and materials assumed in Project Gewähr 1985 (NAGRA 1985a, 1985b, 1985c), which were also used in the Kristallin-I Project (NAGRA 1994a). Reports by KAHR & MÜLLER-VONMOOS (1982), HOPKIRK, GILBY & SCHWANNER (1983), HOPKIRK & WAGNER (1986), NAGRA (1988) and HOPKIRK & ZUIDEMA (1992), together with our experience of thermal analyses, provided supplementary information for the modeling studies. In addition, reports by THUNVIK & BRAESTER (1991) for the Swedish SKB-91 Project and by PNC (1992) for the Japanese H3 analysis were used to support the appropriateness of the selected bentonite material properties.

2.1 Analysis and models

The finite-element analysis program ADINA-T (Automatic Dynamic Incremental Nonlinear Analysis of Temperatures; ROLPH & BATHE 1982) was used for calculating temperatures in this study. Its solution methodology is based on the finite-element formulation of the non-steady-state and non-linear heat flow equations.

In Project Gewähr 1985, temperature distributions were calculated using two models: a two-dimensional model in the tunnel transverse plane (Model 1) and an axial-symmetric model in the tunnel longitudinal plane (Model 2). Our experience of thermal analyses, however, suggests that there are clear differences between the maximum temperatures obtained using these simple models and those obtained using three-dimensional models. Thus, a three-dimensional analysis was conducted in this study.

Heat is transported by one of three mechanisms, namely conduction, convection and radiation (BEAR 1972). HOPKIRK & WAGNER (1986) assumed, for Project Gewähr 1985, that heat is transported solely by conduction, except for air gaps where heat transport is by conduction and radiation. They also noted that radiation in air gaps transmits approximately 80% of the total thermal energy. In spite of the views of HOPKIRK & WAGNER (1986), heat transport in all the components considered in this study is assumed to be solely by conduction, even in air gaps. This ensures an element of conservatism in the temperature calculations; if heat transport were assumed to be solely by conduction, even in air gaps, this would tend to result in higher temperatures in the vitrified waste, the canister and the inner layers of bentonite.

The thermal properties of each material in this study are assumed to be homogeneous and isotropic. Those of the vitrified waste, canister, air and bentonite are further assumed to be temperature-dependent, while those of crystalline rock are assumed to be temperature-independent.

2.2 Geometric modeling and temperature conditions

2.2.1 Canister

Figure 2-1 shows the geometry of the Nagra reference cast steel canister for disposal of vitrified HLW (NAGRA 1985a) and Figure 2-2 shows the simple canister model used in the numerical analyses of this study. The vitrified waste package is 440 mm in diameter and 1200 mm long and the surrounding steel canister has a side-wall thickness of 250 mm. The thin steel fabrication container is ignored in this model.

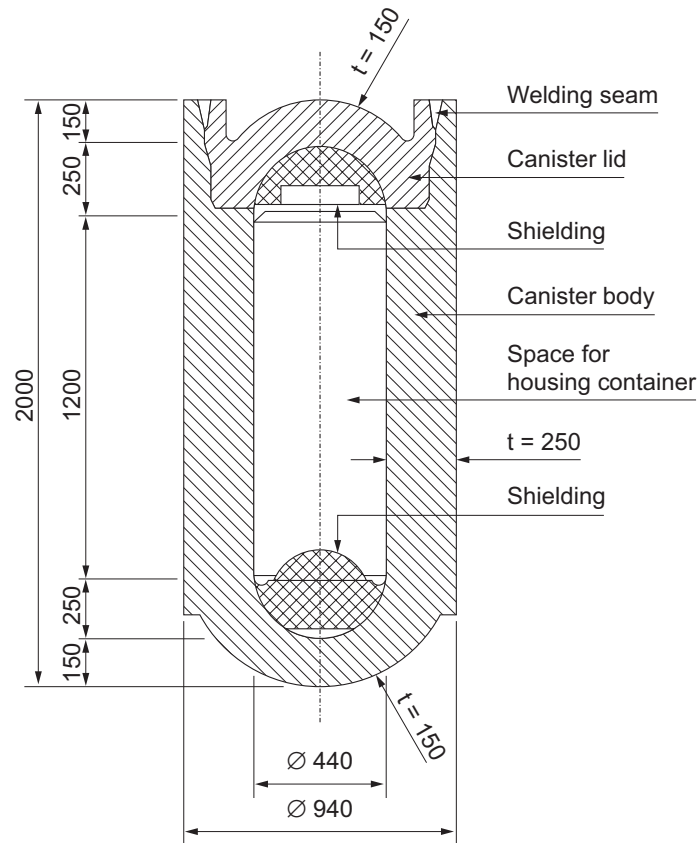


Fig. 2-1: Geometry of the Nagra reference cast steel canister (dimensions in mm; NAGRA 1985a)

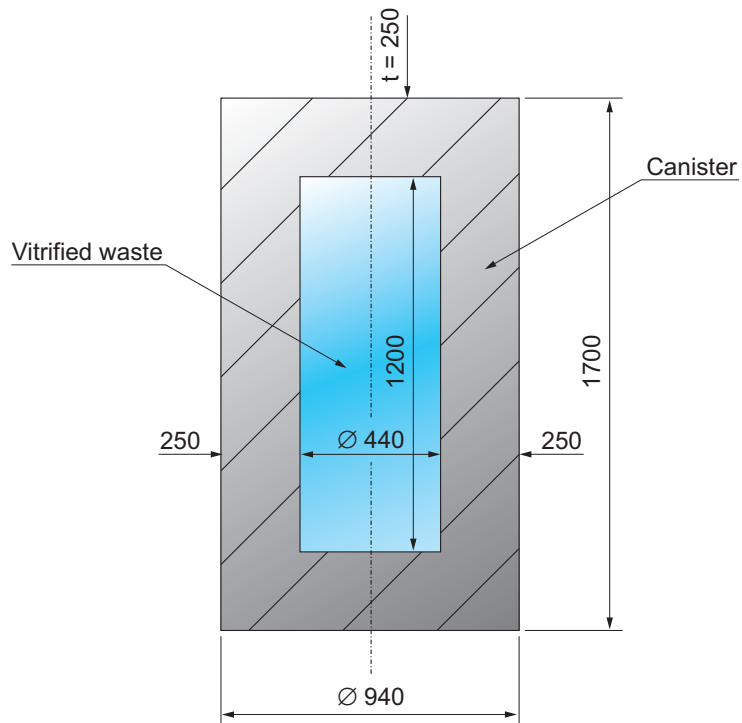


Fig. 2-2: Canister model used for numerical analyses in this study (dimensions in mm)

2.2.2 Emplacement tunnels

This study investigates only a single-level layout option for a repository (NAGRA 1994b). The horizontal spacing of emplacement tunnels (from the center of one tunnel to the center of the next) is varied between 40 m, 20 m and 10 m, as illustrated in Figure 2-3. As specified in Project Gewähr 1985 and the Kristallin-I Project (NAGRA 1985a, 1994a), the diameter of the emplacement tunnels and the longitudinal pitch of the canisters (from center to center) are set to 3.7 m and 5.0 m, respectively.

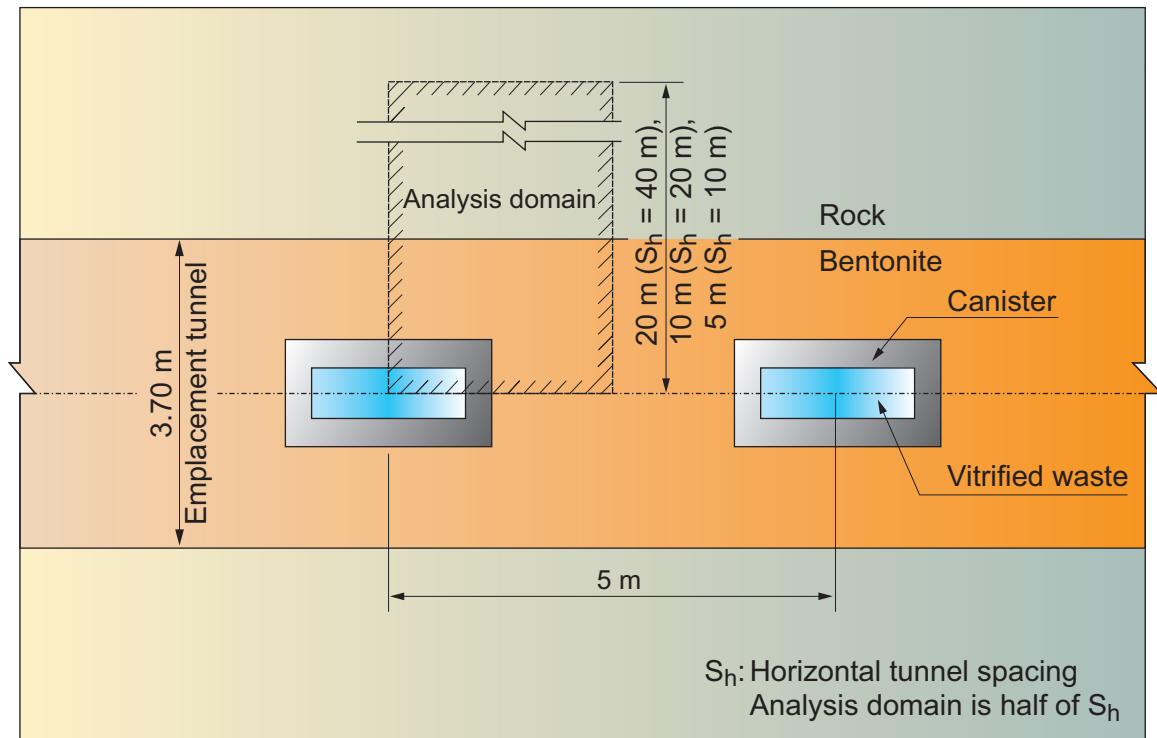


Fig. 2-3: Geometry of a horizontal plane through the near-field for the thermal analyses in this study (originally from NAGRA 1985a)

2.2.3 Depth, initial temperatures and analysis domain

The repository is assumed to be located at a depth of around 1200 m; the ambient rock temperature at this depth is assumed to be 55 °C, which is the same as the value reported by HOPKIRK & WAGNER (1986). The vertical gradient of ambient rock temperature is assumed to be 3 °C/100 m. The initial temperatures of the bentonite and the canister containing the vitrified waste are assumed to be 35 °C and 65 °C, respectively (HOPKIRK & WAGNER 1986).

In Project Gewähr 1985, the vertical domain in the analyses for temperature calculations extended 300 m above and below the repository depth. However, our experience suggests that this vertical domain should be as large as possible to allow constant temperature conditions to be reasonably applied to these top and bottom boundaries. Therefore, the analysis domain in this study is assumed to extend 500 m above and below the 1200 m level, as illustrated in Figure 2-4.

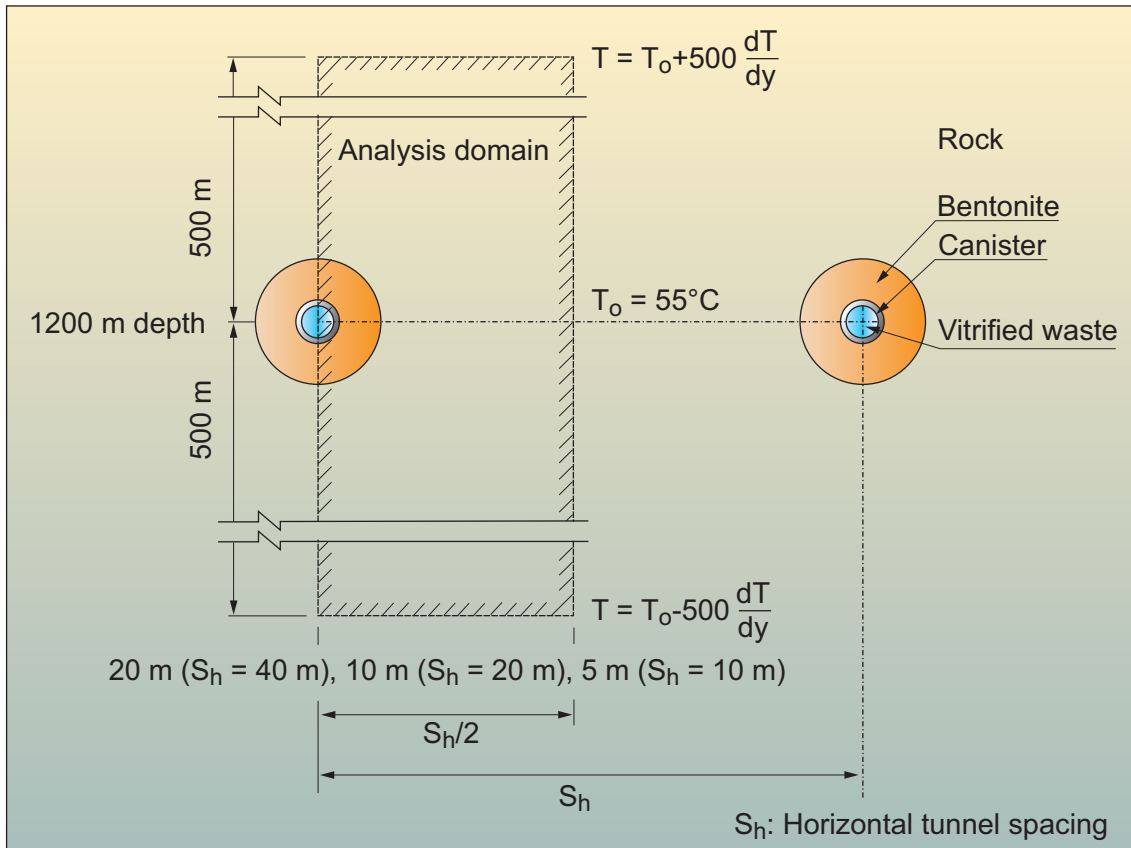


Fig. 2-4: Analysis domain for the thermal analyses in this study (originally from NAGRA 1985a)

2.2.4 Air gaps in the bentonite

In Project Gewähr 1985, three 10 mm thick air gaps were assumed to be located between the canister and the bentonite (A), between the bentonite blocks (B) and between the bentonite and the rock (C) (see Fig. 2-5); these were taken into consideration in the thermal analyses (NAGRA 1985a, 1985b, 1985c). The thermal conductivity of air is so low in comparison with that of either the canister or the bentonite that air gaps function as high-performance insulators which keep the temperatures of inner components high. Although assuming the presence (for all time) of air gaps is likely to be conservative, this assumption is certainly unrealistic, since the high swelling capacity of the compacted bentonite as it saturates will tend to close such gaps. However, considerable uncertainty surrounds the duration and uniformity of the resaturation process and, in order to scope the consequences of this uncertainty, calculations in the present study are made both with and without the presence of air gaps. In calculations where the presence of air gaps is assumed, their number (three), locations and thickness are taken from Project Gewähr 1985.

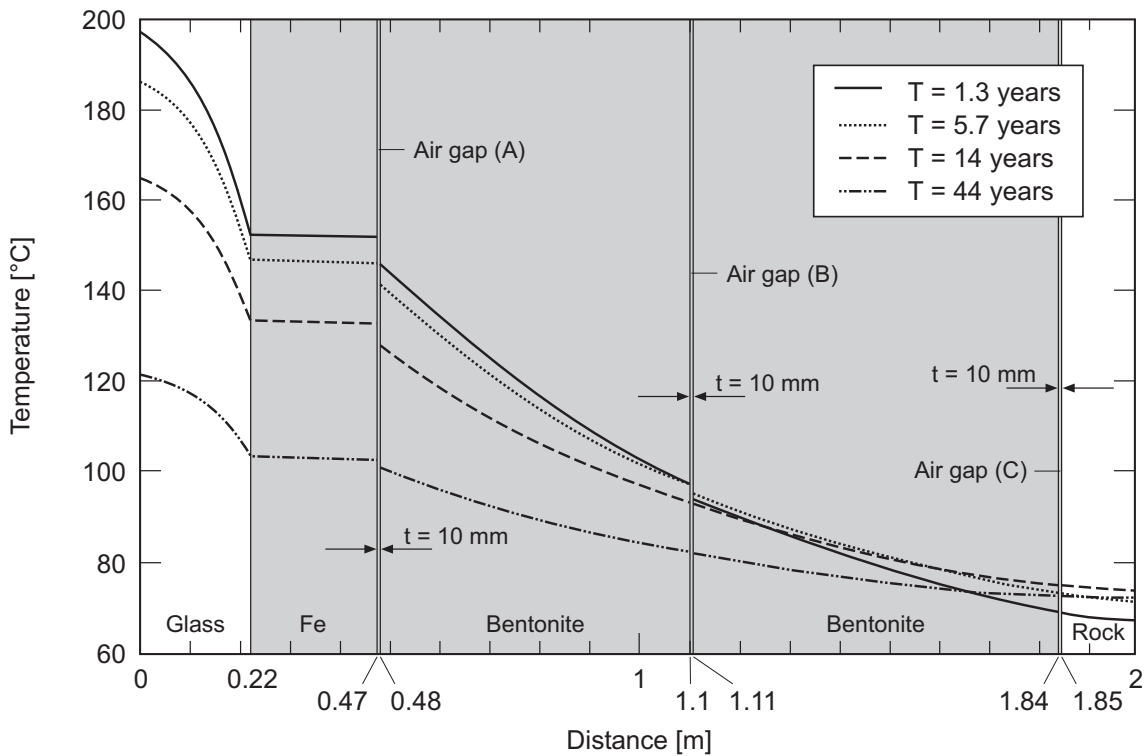


Fig. 2-5: Locations of the three air gaps assumed in Project Gewähr 1985 (originally from NAGRA 1985a)

2.3 Heat production

Initially, vitrified HLW waste generates a large amount of heat due to radioactive decay of short-lived radionuclides. To reduce the resultant temperatures in the repository, the waste will be stored to allow radiogenic heat output to decline. At present, a storage period of at least 40 years is planned between unloading of fuel from the reactors and emplacement of HLW in a repository. The present report assumes a 40-year storage period, as in Project Gewähr 1985 (NAGRA 1985a, 1985b, 1985c). Figure 2-6 shows the heat release rate from a high-level reprocessing waste package versus time as used in the report by HOPKIRK & WAGNER (1986). Table 2-1 gives the heat production values, slightly modified and updated for the Kristallin-I Project (ALDER & MCGINNIS 1993; NAGRA 1994a). The latter values are used in this study.

Tab. 2-1: Heat production values for vitrified waste used in this study (ALDER & MCGINNIS 1993)

Time after fuel unloading [a]	Average heat production [W/canister]
40	589.3
50	468.6
100	161.3
300	21.6
600	12.9
1000	7.3

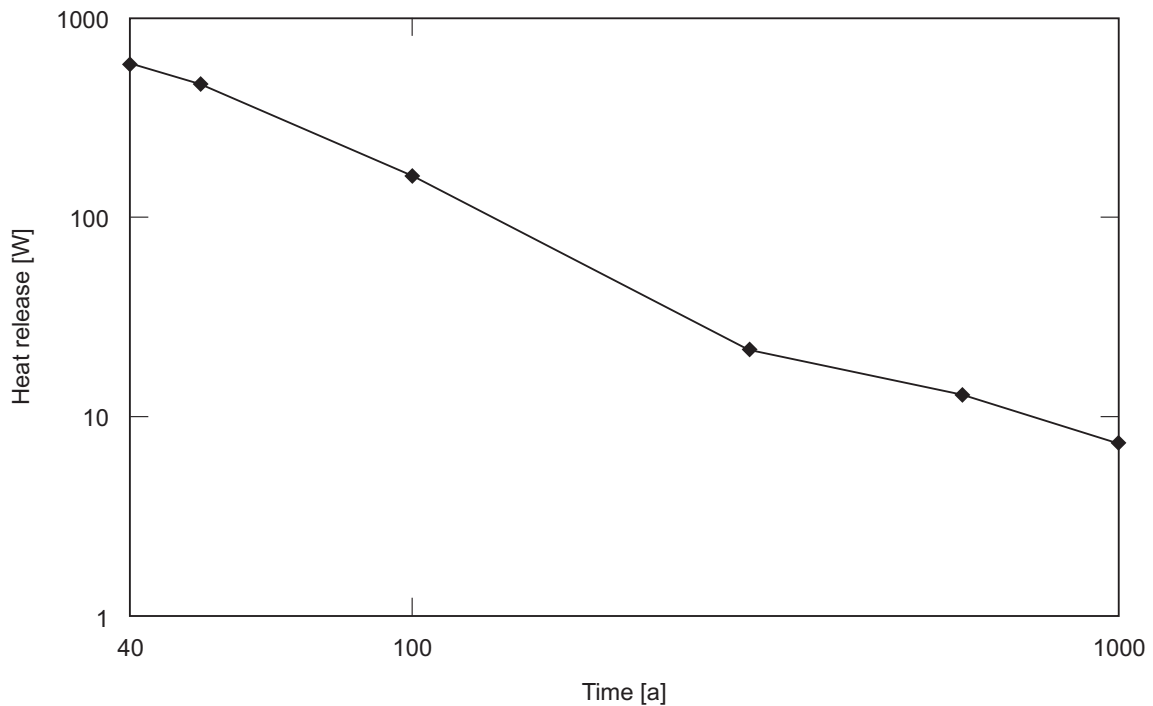


Fig. 2-6: Heat release rate from a high-level reprocessing waste package versus time since unloading of the fuel from the reactor (HOPKIRK & WAGNER 1986)

2.4 Thermal properties of system components

2.4.1 Bentonite

The thermal properties of bentonite depend strongly on the type of bentonite used, as well as on its bulk density, water content and temperature. NAGRA (1985b), HOPKIRK, GILBY & SCHWANNER (1983) and HOPKIRK & WAGNER (1986) used the following equations to represent the thermal properties of compacted sodium bentonite blocks considered as a potential backfill material for emplacement tunnels in a HLW repository.

$$\rho_b = \rho_{\text{dry}} (1 + 0.01 \phi) \dots (2.1)$$

$$k_b = 0.60 (\rho_b - 1) + 0.004 \phi \rho_b^3 + 0.01 \sqrt{T} \dots (2.2)$$

$$C_b = \frac{\rho_b}{1 + 0.01 \phi} (0.01 \phi \times C_w + C_s) \dots (2.3)$$

where	ρ_{dry}	bulk density of dry bentonite (assumed to be 1.635 g/cm ³ in this study)
	ρ_b	bulk density of wet bentonite [g/cm ³]
	ϕ	water content [% by weight]
	k_b	thermal conductivity of bentonite [W/mK]
	T	temperature [°C]
	C_b	heat capacity of bentonite [MJ/m ³ K]
	C_w	heat capacity of water (= 4.2 kJ/kgK)
	C_s	heat capacity of dry bentonite (= 0.8 – 1.05 kJ/kgK; conservatively assumed to be 0.8 kJ/kgK in this study)

Using equations (2.1), (2.2) and (2.3), Table 2-2 gives the thermal conductivities and heat capacities of bentonite blocks as functions of temperature and water content.

Tab. 2-2: Thermal properties of bentonite blocks

Temperature	Thermal conductivity [W/mK]		
	for 0% water content [% by weight]	for 2% water content [% by weight]	for 7% water content [% by weight]
30	0.436	0.493	0.654
40	0.444	0.501	0.662
60	0.458	0.515	0.677
80	0.470	0.527	0.689
100	0.481	0.538	0.699
120	0.491	0.547	0.709
140	0.499	0.556	0.718
150	0.503	0.560	0.722
	Heat capacity [MJ/m ³ K]		
	1.308	1.446	1.788

It is difficult to predict the time-dependent water content of bentonite blocks after closure of a repository, because the initial content will be altered by the simultaneous effects of drying-out due to build-up of high temperatures, uptake of groundwater from the outside and swelling. A simplified near-field scenario, which describes time-dependent bentonite water content, is therefore needed to determine the thermal properties of bentonite blocks.

Table 2-3 provides an international cross-comparison of bentonite thermal properties employed for various HLW projects. Use of the constant thermal properties employed by SKB and PNC is a practical compromise, which may provide a good estimate of temperatures in the development of a repository concept, because it is difficult to predict time history of bentonite water content. However, the Nagra scenario, which assumes time-dependent thermal properties of bentonite, is probably more realistic.

Tab. 2-3: Cross-comparison of bentonite thermal properties

Organization (Country)	Thermal conductivity [W/mK]	Heat capacity [MJ/m ³ K]	Remarks
SKB (Sweden)	0.75 (dry)	2.2 (dry)	Constant values THUNVIK & BRAESTER (1991)
PNC (Japan)	0.9 (dry) 1.7 (saturated)	1.14 (dry) 2.1 (saturated)	Constant values PNC (1992)
Nagra (Switzerland)	0.511 – 0.646	1.635 – 2.091	Dependent on temperature and water content HOPKIRK & WAGNER (1986)

Thus, three cases of bentonite thermal properties are defined and investigated in this study: the first is the variable case which follows Nagra's concept of analysis; the second is the constant case which assumes constant water content; and the third is the bounding case which assumes three kinds of bounding properties.

- 1) Variable case: Initially $\phi = 7\%$, then $\phi = 2\%$ at $100\text{ }^{\circ}\text{C}$ and, finally, $\phi = 0\%$ at $150\text{ }^{\circ}\text{C}$ (see Fig. 2-7)
- 2) Constant case: Constant water content $\phi = 2\%$
- 3) Bounding cases:
 - a) Thermal conductivity 0.7 W/mK , heat capacity $1.1\text{ MJ/m}^3\text{K}$
 - b) Thermal conductivity 1.7 W/mK , heat capacity $2.1\text{ MJ/m}^3\text{K}$
 - c) Thermal conductivity 0.7 W/mK , heat capacity $2.1\text{ MJ/m}^3\text{K}$

The thermal properties of bentonite blocks assumed for the numerical analyses in this study are summarized in Table 2-4.

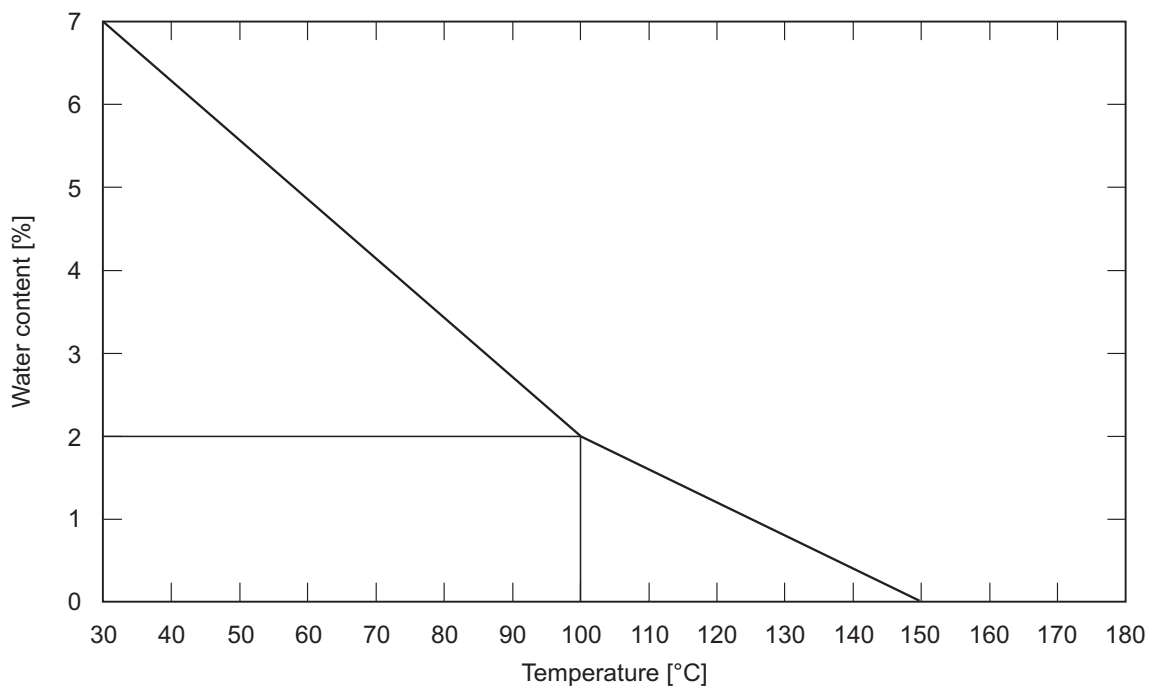


Fig. 2-7: Water content of bentonite as a function of temperature (HOPKIRK & WAGNER 1986)

Tab. 2-4: Thermal properties of bentonite for this study

Temperature [°C]	Variable case ($\phi = 7$ to 0%)		Constant case ($\phi = 2\%$)		Bounding cases (constant parameters)	
	Thermal conductivity [W/mK]	Thermal capacity [MJ/m ³ K]	Thermal conductivity [W/mK]	Thermal capacity [MJ/m ³ K]	Thermal conductivity [W/mK]	Thermal capacity [MJ/m ³ K]
30	0.654 (7%)	1.788	0.493	1.446		
40	0.638 (6.3%)	1.741	0.501	1.446		
60	0.605 (4.9%)	1.644	0.515	1.446		
80	0.570 (3.4%)	1.542	0.527	1.446		
100	0.538 (2%)	1.446	0.538	1.446		
120	0.524 (1.2%)	1.391	0.547	1.446		
140	0.511 (0.4%)	1.336	0.556	1.446		
150	0.503 (0%)	1.308	0.560	1.446		
					0.7	1.1
					1.7	2.1
					0.7	2.1

2.4.2 Other components

Table 2-5 summarizes the thermal properties of the other near-field components for the numerical analyses in this study, which are basically the same as those used in Project Gewähr 1985 (NAGRA 1985a, 1985b, 1985c) and in the reports by HOPKIRK, GILBY & SCHWANNER (1983) and HOPKIRK & WAGNER (1986). The input data given in Table 2-5 for the analyses in this study are interpolated linearly between the discrete values depending on temperatures.

As noted in section 2.1, the air gaps in this study are modeled as heat-conducting material with the thermal properties of air, which means that heat transport is assumed to be solely by conduction in such gaps.

Tab. 2-5: Thermal properties of the other components for this study

Material	Thermal conductivity [W/mK]	Thermal capacity [MJ/m ³ K]
Vitrified waste	1.0 at 30 °C	3.0
	1.1 at 150 °C	3.0
	1.2 at 250 °C	3.0
Canister	54.0 at 0 °C	3.05
	52.0 at 100 °C	3.05
	46.0 at 300 °C	3.05
Air ^{*2)}	2.41×10^{-2} at 0 °C ^{*1)}	1.212×10^{-3} at 20 °C ^{*1)}
	3.17×10^{-2} at 100 °C ^{*1)}	9.56×10^{-4} at 100 °C ^{*1)}
	7.60×10^{-2} at 1000 °C ^{*1)}	5.44×10^{-4} at 500 °C ^{*1)}
Crystalline rock	2.5	2.3

^{*1)} These values are obtained from the report by JAO (1991)

^{*2)} Heat is transported solely by conduction in air gaps

2.5 Schematic representation of the model and boundary conditions

Figure 2-8 shows a schematic illustration of the model used for the three-dimensional numerical analyses in this study. The vertical sides of the model are all assumed to be zero-flux boundaries and the top and bottom sides of the model are constant temperature boundaries. Figure 2-9 shows a model geometry of the near-field and Figure 2-10 illustrates one example of the three-dimensional finite-element meshes used in this study.

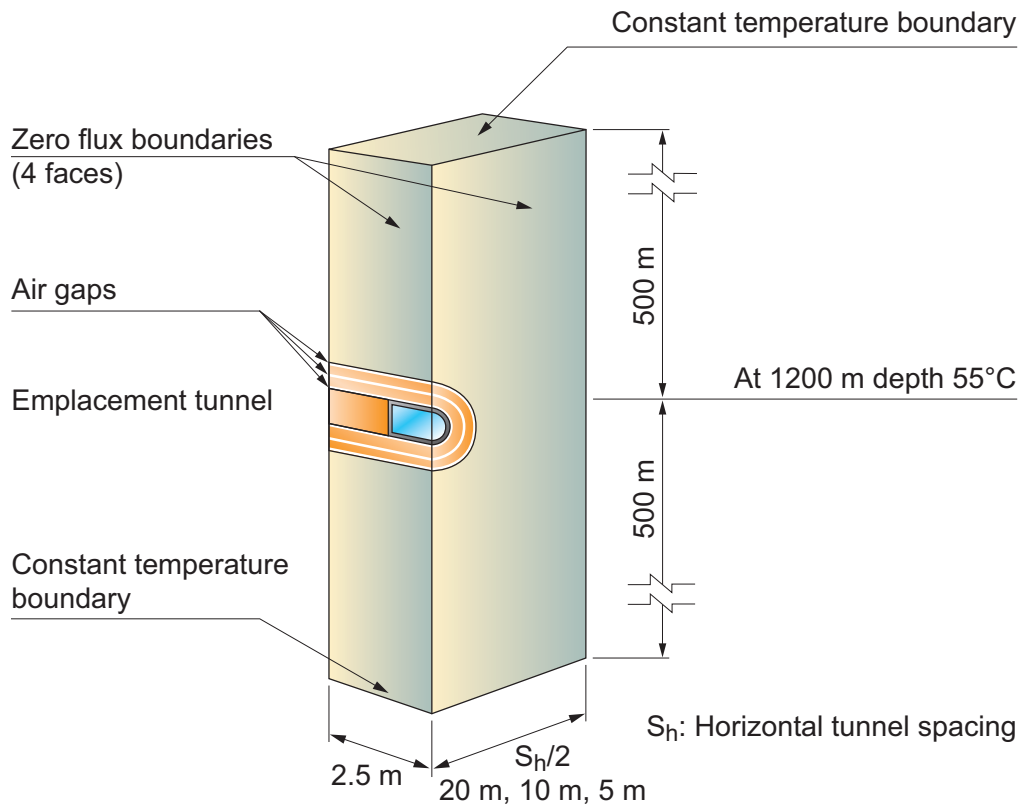


Fig. 2-8: Three-dimensional model representation and boundary conditions

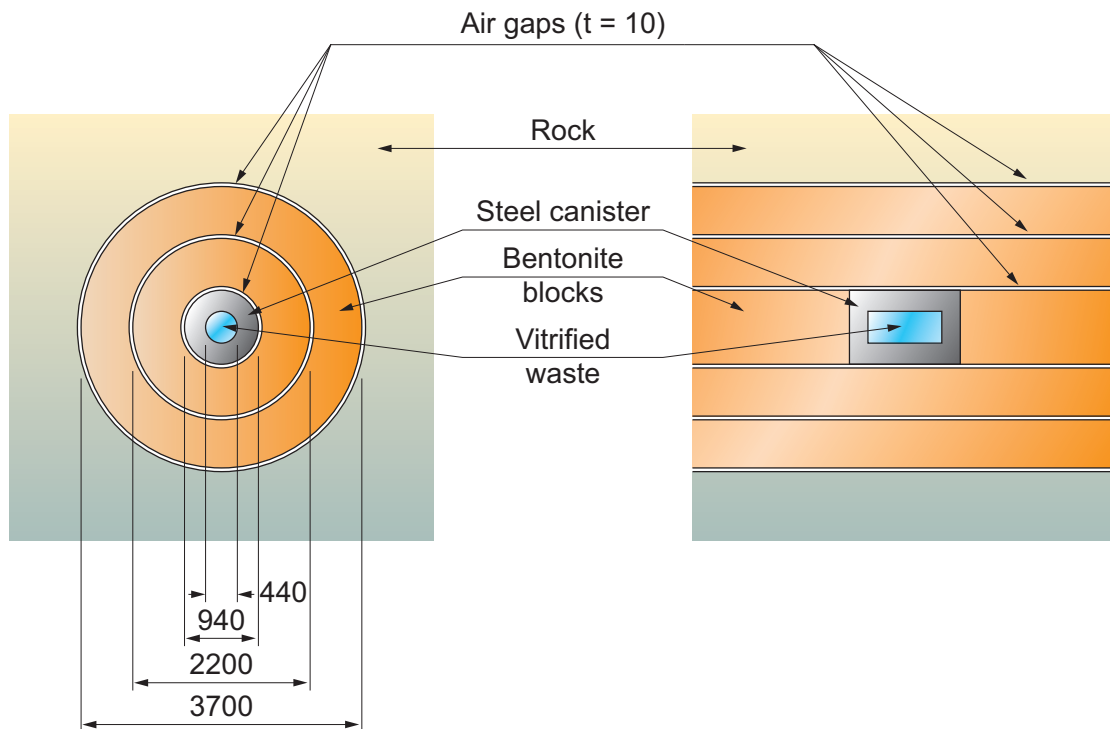


Fig. 2-9: Model geometry of the near-field around a tunnel (dimensions in mm)

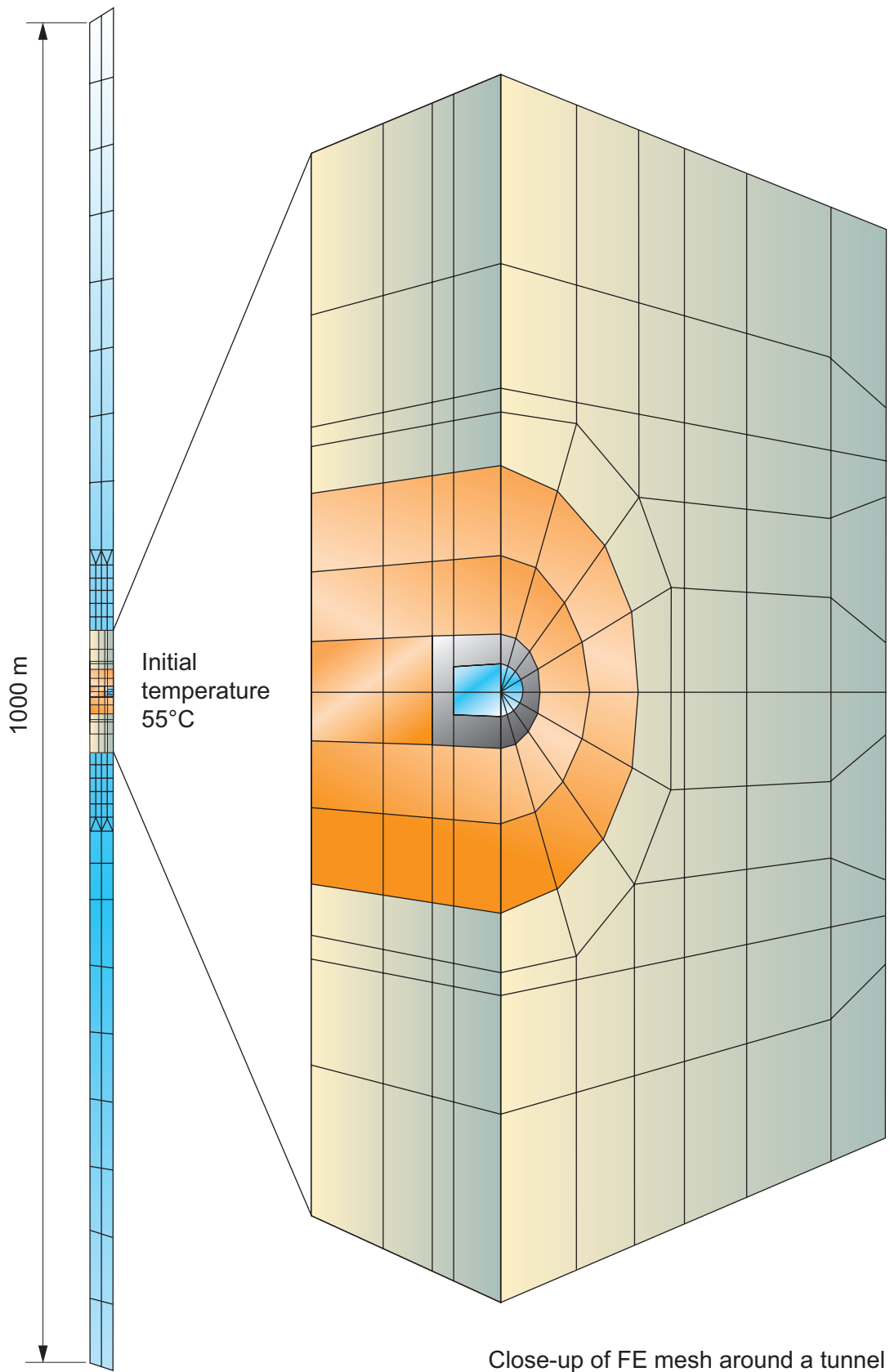


Fig. 2-10: Example of the three-dimensional finite-element mesh used in this study

2.6 Variable parameters selected for the numerical analyses in this study

The key parameters varied for the numerical analyses are noted below and summarized in Table 2-6.

- 1) Horizontal spacing of emplacement tunnels [$S_h = 40$ m, 20 m, 10 m]
- 2) Thermal properties of bentonite [variable case $\phi = 7 - 0\%$, constant case $\phi = 2\%$, bounding cases a), b) and c)]
- 3) Existence of three air gaps

Tab. 2-6: Parameters selected for the numerical analyses in this study

Analysis no.	Air gap	Thermal properties of bentonite	Horizontal tunnel spacing S_h [m]
1	Yes	Variable case ($\phi = 7 - 0\%$)	40
2			20
3			10
4	Yes	Constant case ($\phi = 2\%$)	40
5			20
6			10
7	No	Variable case ($\phi = 7 - 0\%$)	40
8			20
9			10
10	No	Bounding case a)	20
11		Bounding case b)	
12		Bounding case c)	

3 Calculated temperature distributions

In this chapter, the near-field temperature distributions calculated in the numerical analyses are presented. First, the maximum temperatures of each component are given, then temperature profiles and time histories for each analysis case are shown. Finally, the temperature distributions are compared from the following viewpoints:

- 1) Comparison with the results in Project Gewähr 1985
- 2) Effect of tunnel spacing
- 3) Effect of bentonite thermal properties
- 4) Effect of air gaps

3.1 Maximum temperatures of each component

Table 3-1 gives the maximum temperature in degrees Celsius [$^{\circ}\text{C}$] calculated for Analyses No. 1 to 12, together with its time of occurrence after emplacement of the canister in the tunnel.

It can be seen from Table 3-1 that the maximum temperature of each component increases very little between tunnel spacing $S_h = 40$ m and $S_h = 20$ m, but increases significantly between $S_h = 20$ m and $S_h = 10$ m. For example, the maximum temperature of bentonite is 148.2 $^{\circ}\text{C}$ in Analysis No. 1 ($S_h = 40$ m), 149.6 $^{\circ}\text{C}$ in Analysis No. 2 ($S_h = 20$ m) and 166.9 $^{\circ}\text{C}$ in Analysis No. 3 ($S_h = 10$ m). Figure 3-1 shows the relationship between the horizontal tunnel spacing and the maximum temperature of bentonite.

The same trend is also observed for the maximum temperatures of other components (vitrified waste, steel canister and rock) in all analysis cases. The important conclusion to be drawn from this is that a minimum spacing of emplacement tunnels of around 20 m should be selected to ensure that interaction between tunnels will not significantly influence maximum temperatures. The effect of tunnel separation on temperature evolution is discussed further in section 3.4. The following observations can also be made on the results in Table 3-1; these points are discussed in more detail in sections 3.5 and 3.6.

- 1) The maximum temperatures are similar for both variable-case and constant-case thermal properties of bentonite.
- 2) The maximum temperatures in the inner parts of the near-field are reduced in the absence of air gaps, while the temperature at the bentonite-rock interface is very slightly increased.
- 3) The maximum temperatures are insensitive to the thermal conductivity of bentonite over the range examined.
- 4) The maximum temperatures are reduced, particularly in the inner parts of the near-field, if the thermal conductivity is increased.

Tab. 3-1: Maximum temperatures [°C] in various components and their time of occurrence after emplacement

Analysis No.	Temperature in vitrified waste [°C] (Time [a])	Temperature in steel canister [°C] (Time [a])	Temperature in bentonite [°C] (Time [a])	Temperature in rock [°C] (Time [a])
1	226.64 (1.0)	167.90 (1.5)	148.16 (2.0)	73.50 (10)
2	226.98 (1.5)	168.51 (2.0)	149.58 (8.0)	81.85 (40)
3	233.59 (8.0)	183.58 (10)	166.93 (10)	104.89 (40)
4	226.82 (1.0)	167.72 (1.5)	147.73 (2.0)	73.53 (10)
5	226.92 (1.0)	168.06 (2.0)	148.36 (2.0)	81.87 (40)
6	230.58 (7.0)	180.06 (10)	163.25 (10)	104.02 (40)
7	198.86 (1.5)	138.89 (2.0)	137.96 (2.0)	73.71 (10)
8	199.28 (1.5)	141.69 (9.0)	140.87 (9.0)	81.95 (40)
9	210.61 (10)	159.84 (10)	159.02 (10)	104.98 (40)
10	185.94 (1.5)	128.30 (10)	127.50 (10)	81.98 (40)
11	154.84 (2.0)	100.29 (10)	99.48 (10)	81.47 (50)
12	185.26 (1.5)	128.06 (10)	127.26 (10)	81.89 (40)

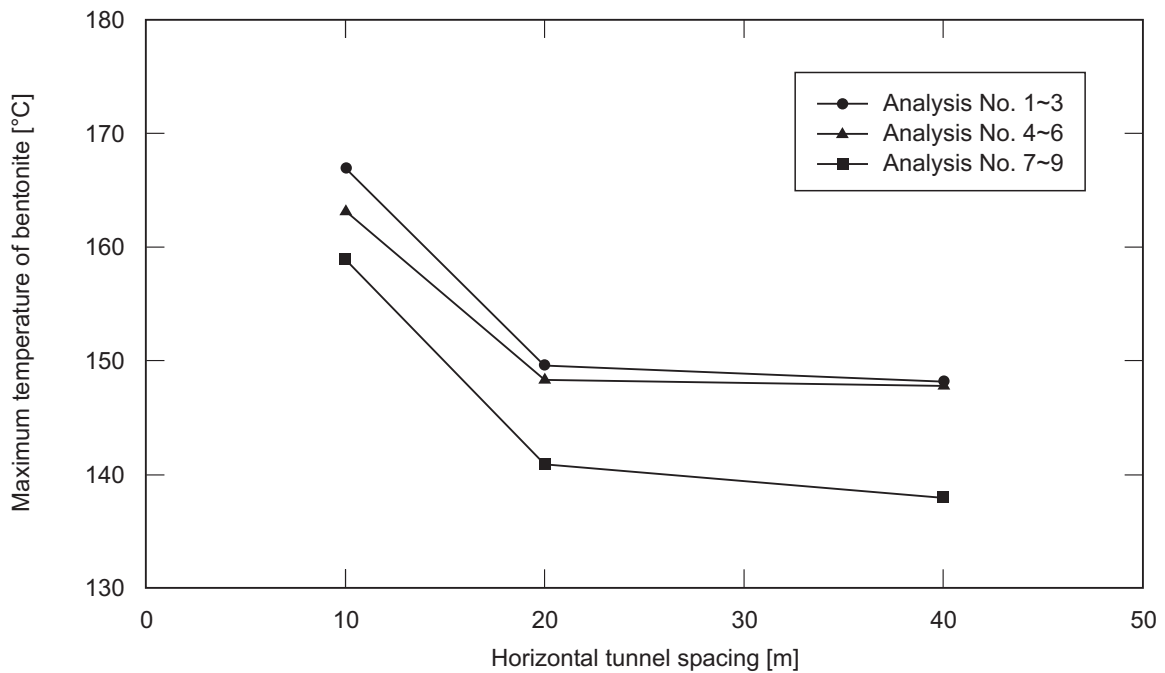


Fig. 3-1: Relationship between horizontal tunnel spacing and maximum temperature of bentonite

3.2 Temperature profiles and temperature-time histories

In this section, the temperature profiles and temperature-time histories calculated for each analysis case are presented.

All numerical calculations in this study were performed on the engineering work-stations located at the Tokyo headquarters of the Obayashi Corporation, allowing the numerical results to be represented as color contour illustrations. Figure 3-2 shows examples of color contours for temperature distributions around a tunnel in Analysis No. 1, indicating times of 1, 10, 40 and 100 years after the emplacement of a canister, respectively. It can be seen that heat spreads out rapidly between 1 and 10 years after emplacement and, after that, the temperatures in the central area decrease with time.

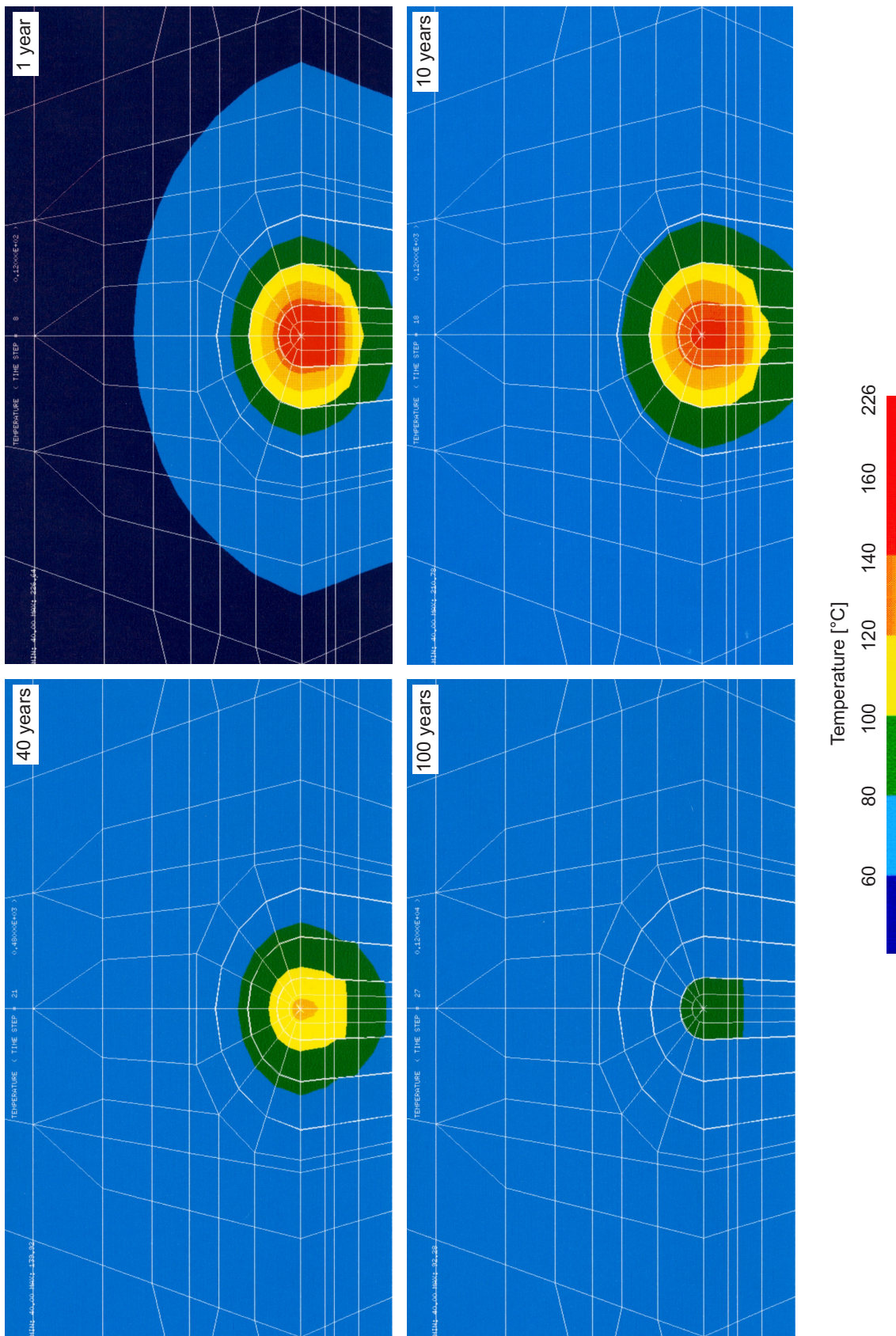


Fig. 3-2: Temperatures for Analysis No. 1 at 1, 10, 40 and 100 years after emplacement

Figure 3-3 shows the temperature output locations A, B, C, D, E, F, G, H and I, extending in a radial direction from the axis of the model, and locations A, J, K, L and M, extending along the axis. In the following, these definitions of output location will be used for the sake of brevity.

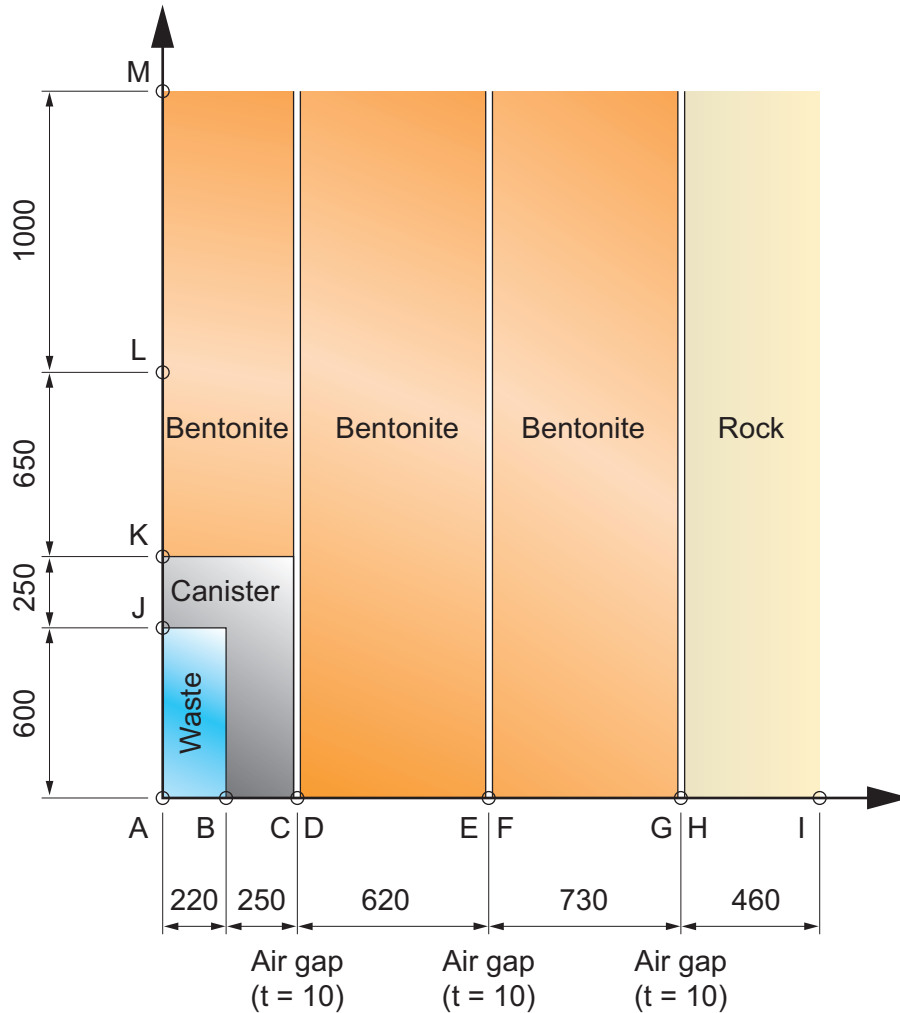


Fig. 3-3: Location of the temperature output points A to M (dimensions in mm)

The top graph in Figure 3-4 shows the temperature profiles of Analysis No. 1 in a radial direction from the center at the indicated times, which include the times of the maximum temperatures of each component as summarized in Table 3-1. The middle and bottom graph in Figure 3-4 show the temperature-time history curves of Analysis No. 1 at the locations indicated in radial and longitudinal direction, respectively. Next, the three graphs of Figure 3-5 show the same information for Analysis No. 2. Similarly, Figures 3-6 to 3-15 show the same information for Analyses No. 3, 4, 5, 6, 7, 8, 9, 10, 11 and 12, respectively.

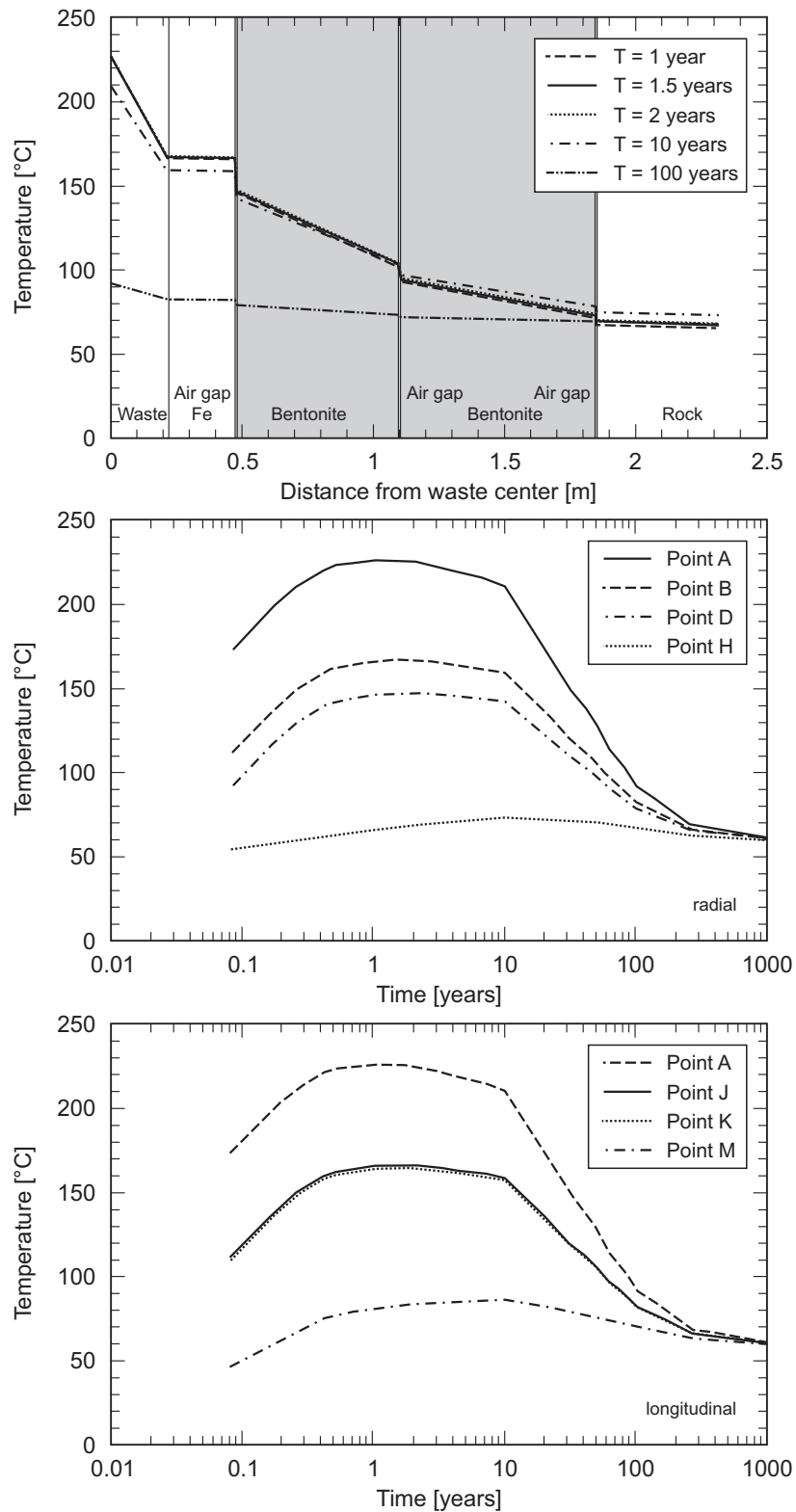


Fig. 3-4: Temperature profiles and temperature-time histories of Analysis No. 1

Top: Temperature profile in a radial direction from the center at the indicated times. Middle and bottom: Temperature-time histories in radial and longitudinal direction, respectively, at the indicated locations.

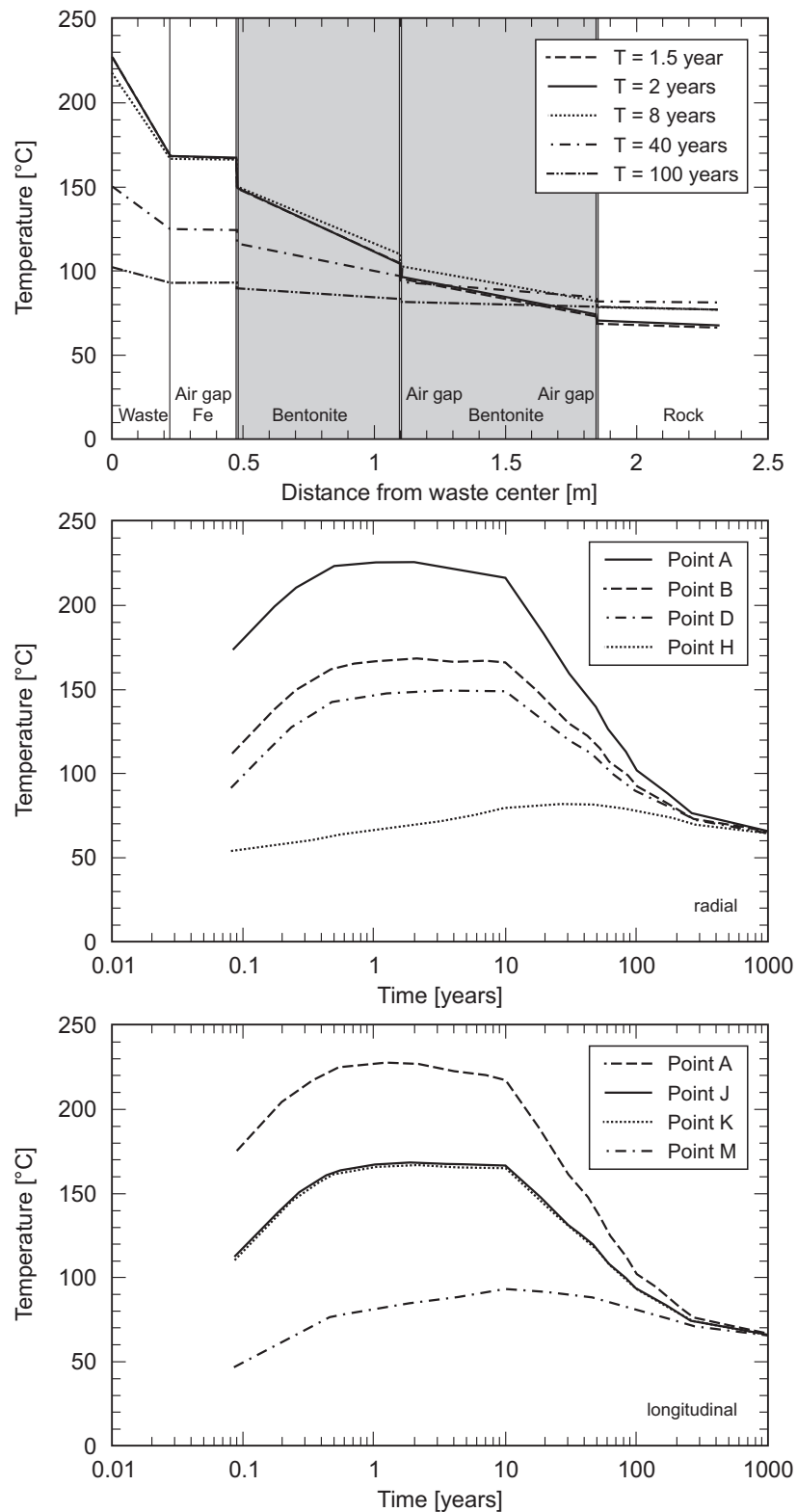


Fig. 3-5: Temperature profiles and temperature-time histories of Analysis No. 2

Top: Temperature profile in a radial direction from the center at the indicated times. Middle and bottom: Temperature-time histories in radial and longitudinal direction, respectively, at the indicated locations.

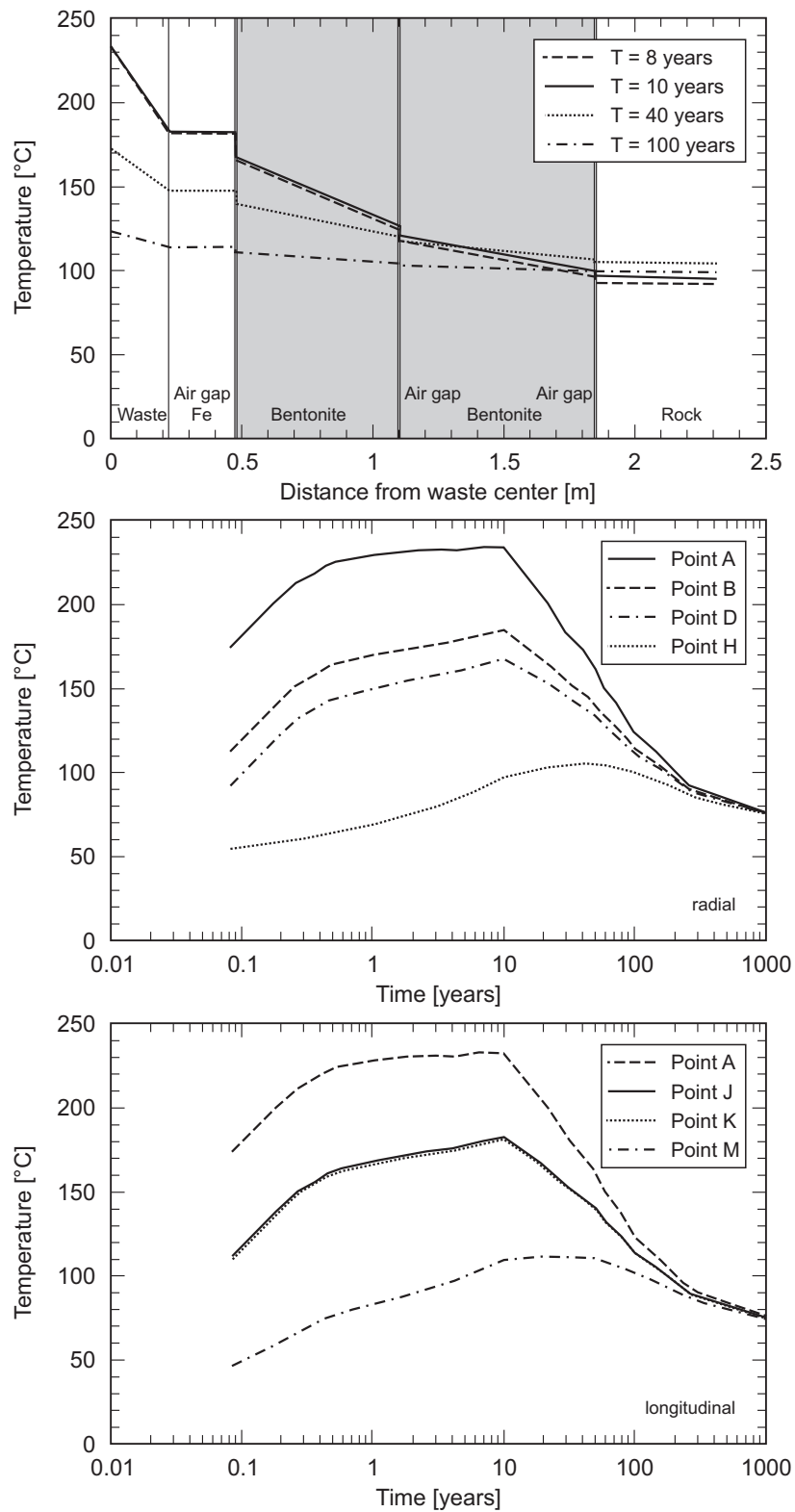


Fig. 3-6: Temperature profiles and temperature-time histories of Analysis No. 3
 Top: Temperature profile in a radial direction from the center at the indicated times. Middle and bottom: Temperature-time histories in radial and longitudinal direction, respectively, at the indicated locations.

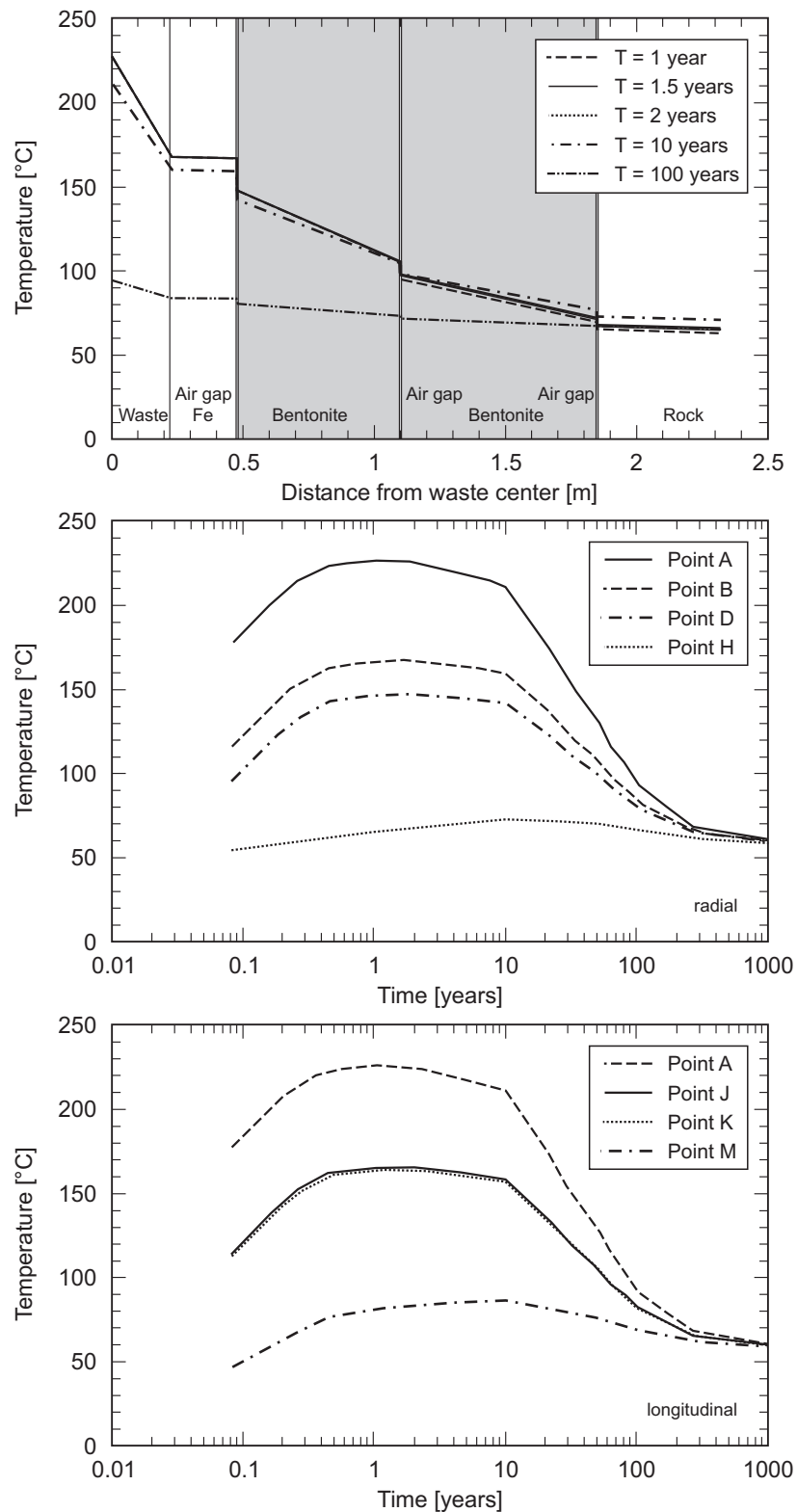


Fig. 3-7: Temperature profiles and temperature-time histories of Analysis No. 4

Top: Temperature profile in a radial direction from the center at the indicated times. Middle and bottom: Temperature-time histories in radial and longitudinal direction, respectively, at the indicated locations.

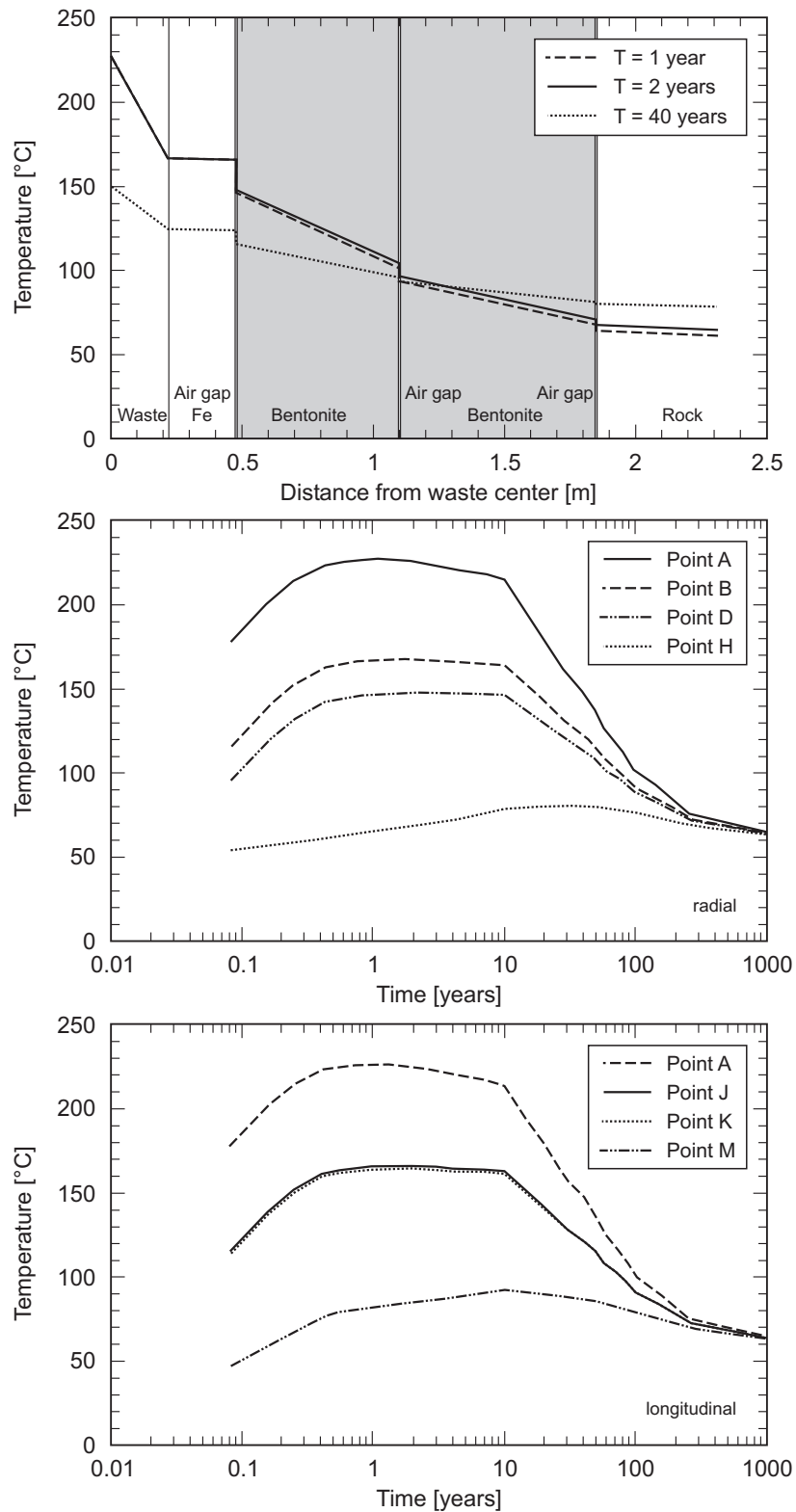


Fig. 3-8: Temperature profiles and temperature-time histories of Analysis No. 5
 Top: Temperature profile in a radial direction from the center at the indicated times. Middle and bottom: Temperature-time histories in radial and longitudinal direction, respectively, at the indicated locations.

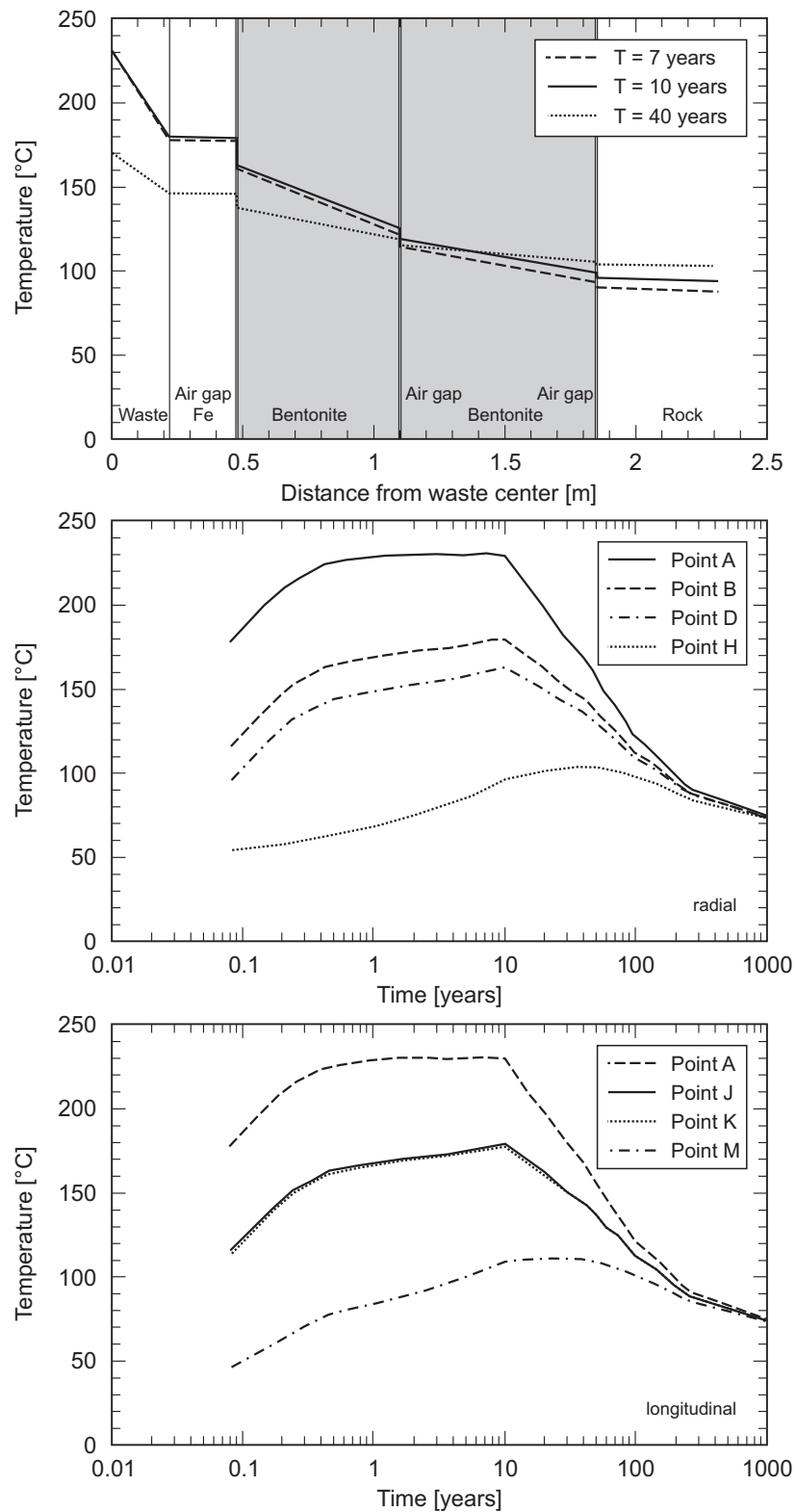


Fig. 3-9: Temperature profiles and temperature-time histories of Analysis No. 6

Top: Temperature profile in a radial direction from the center at the indicated times. Middle and bottom: Temperature-time histories in radial and longitudinal direction, respectively, at the indicated locations.

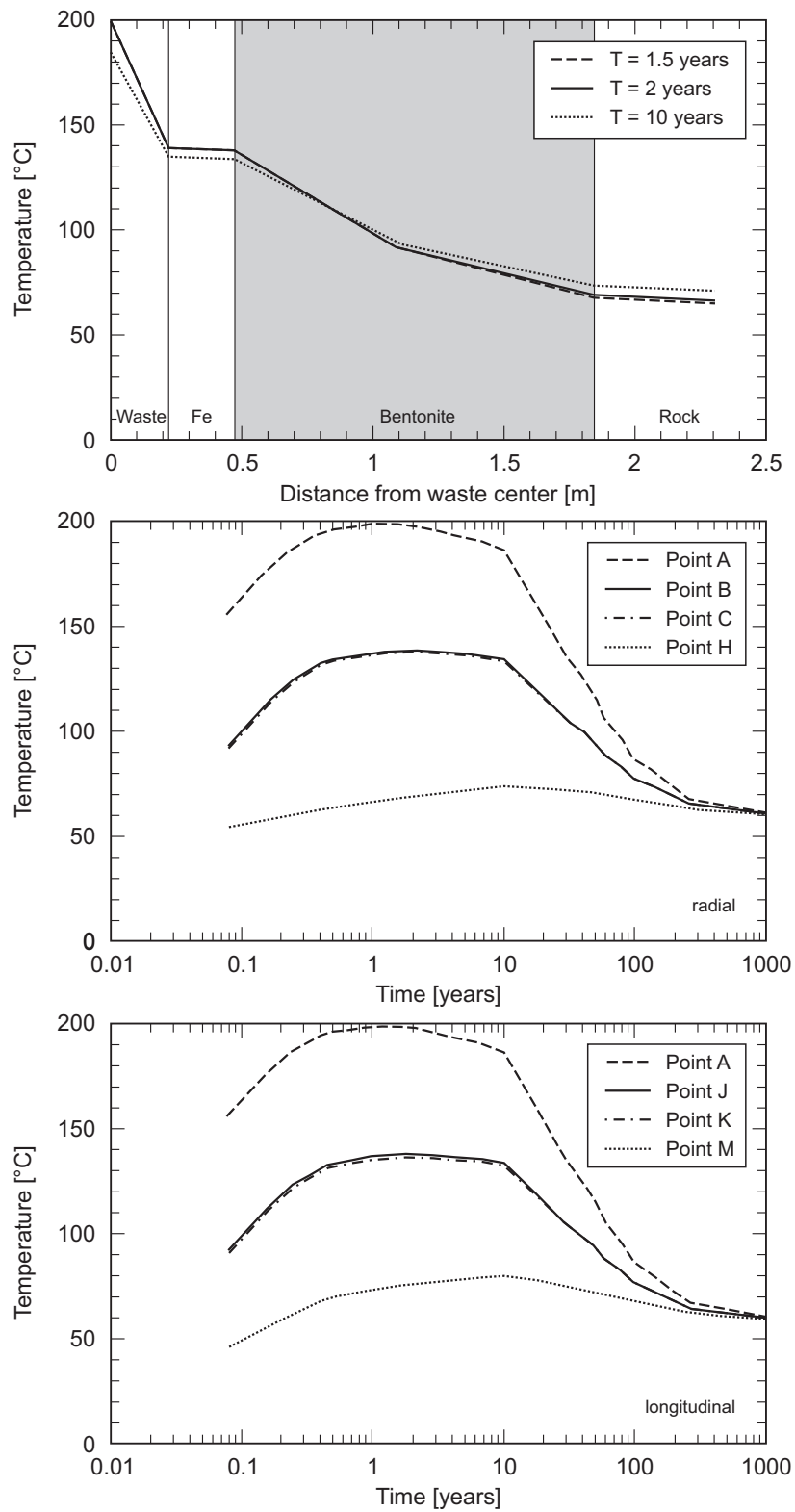


Fig. 3-10: Temperature profiles and temperature-time histories of Analysis No. 7

Top: Temperature profile in a radial direction from the center at the indicated times. Middle and bottom: Temperature-time histories in radial and longitudinal direction, respectively, at the indicated locations.

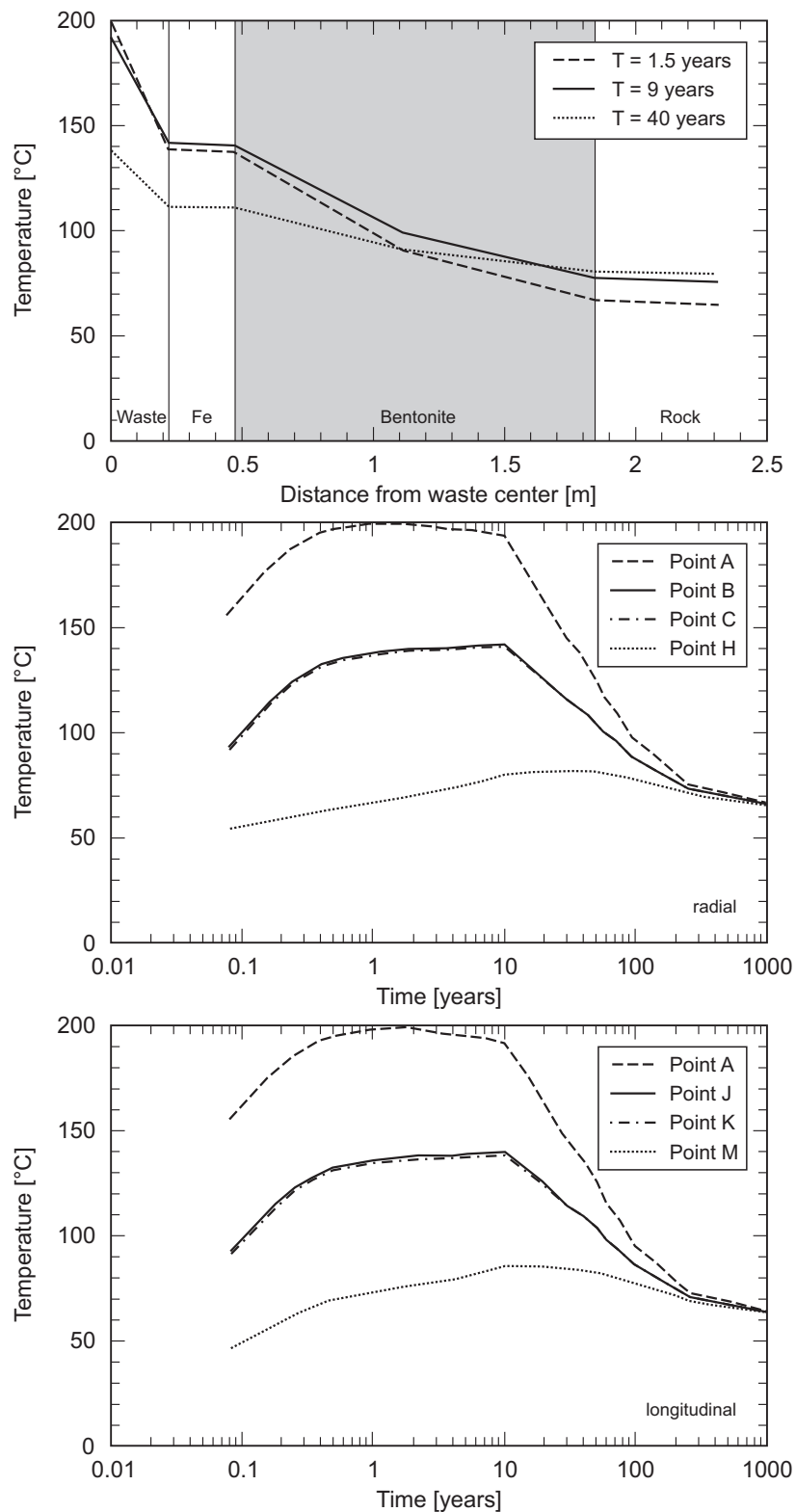


Fig. 3-11: Temperature profiles and temperature-time histories of Analysis No. 8

Top: Temperature profile in a radial direction from the center at the indicated times. Middle and bottom: Temperature-time histories in radial and longitudinal direction, respectively, at the indicated locations.

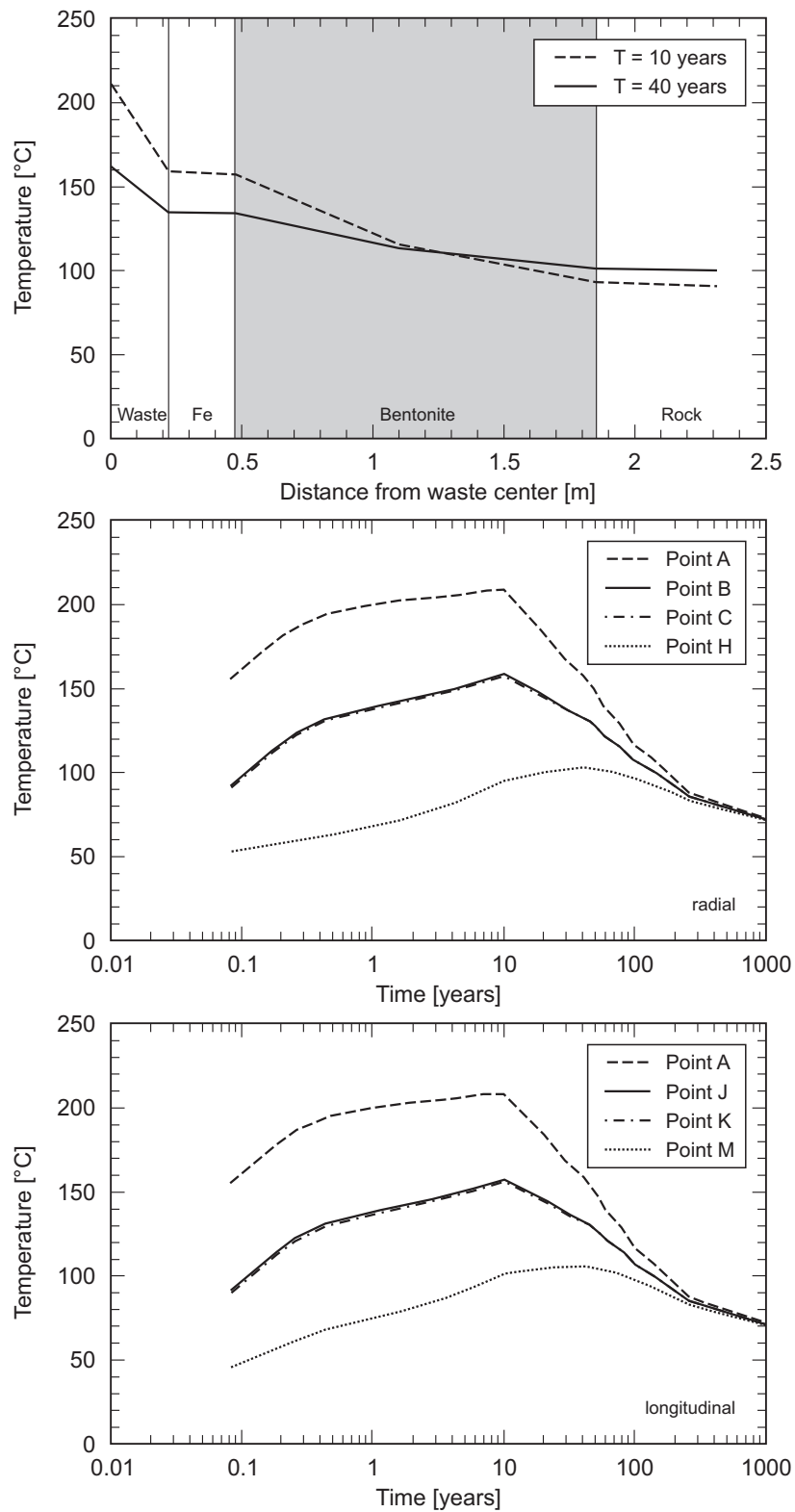


Fig. 3-12: Temperature profiles and temperature-time histories of Analysis No. 9

Top: Temperature profile in a radial direction from the center at the indicated times. Middle and bottom: Temperature-time histories in radial and longitudinal direction, respectively, at the indicated locations.

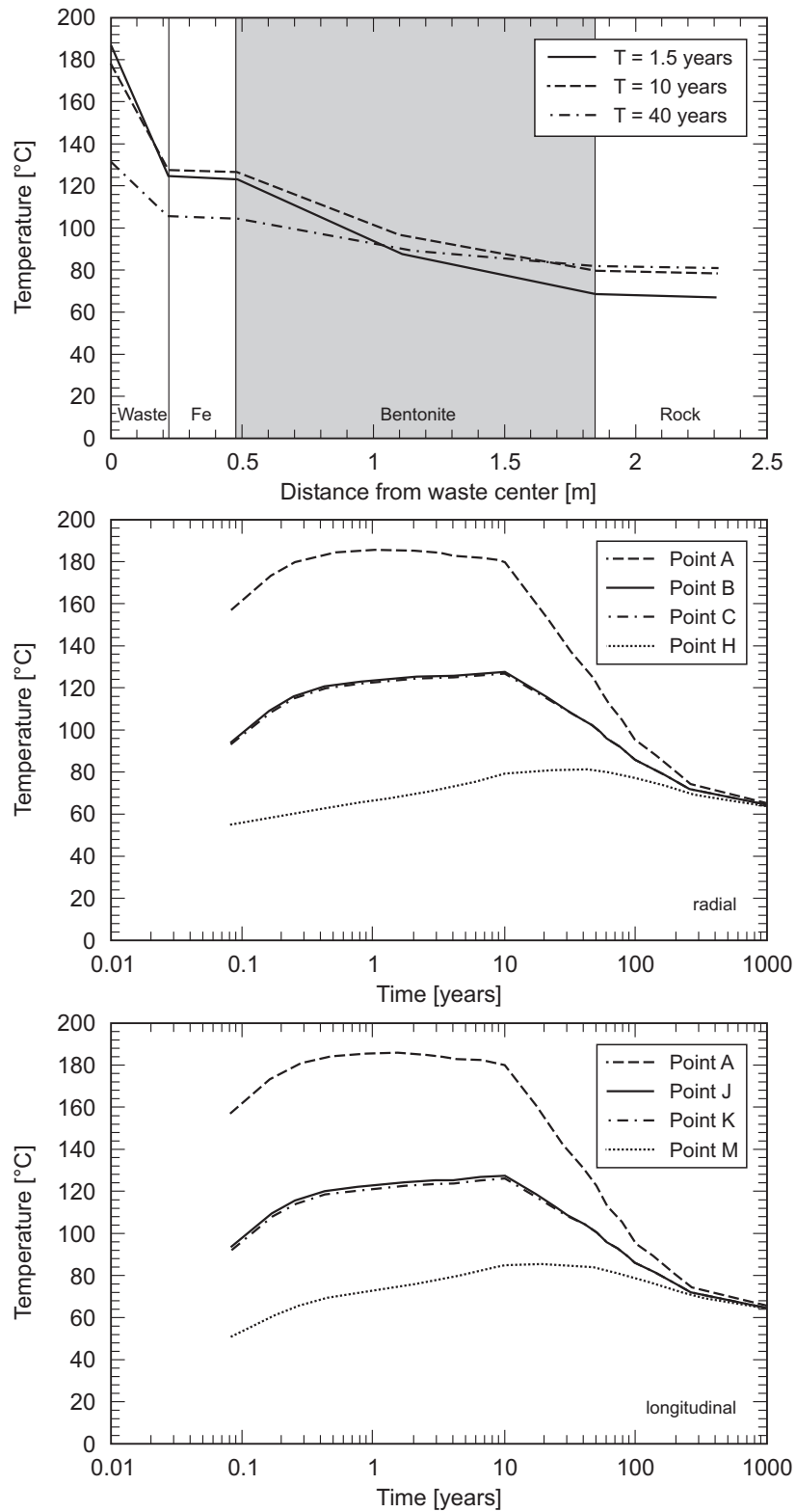


Fig. 3-13: Temperature profiles and temperature-time histories of Analysis No. 10

Top: Temperature profile in a radial direction from the center at the indicated times. Middle and bottom: Temperature-time histories in radial and longitudinal direction, respectively, at the indicated locations.

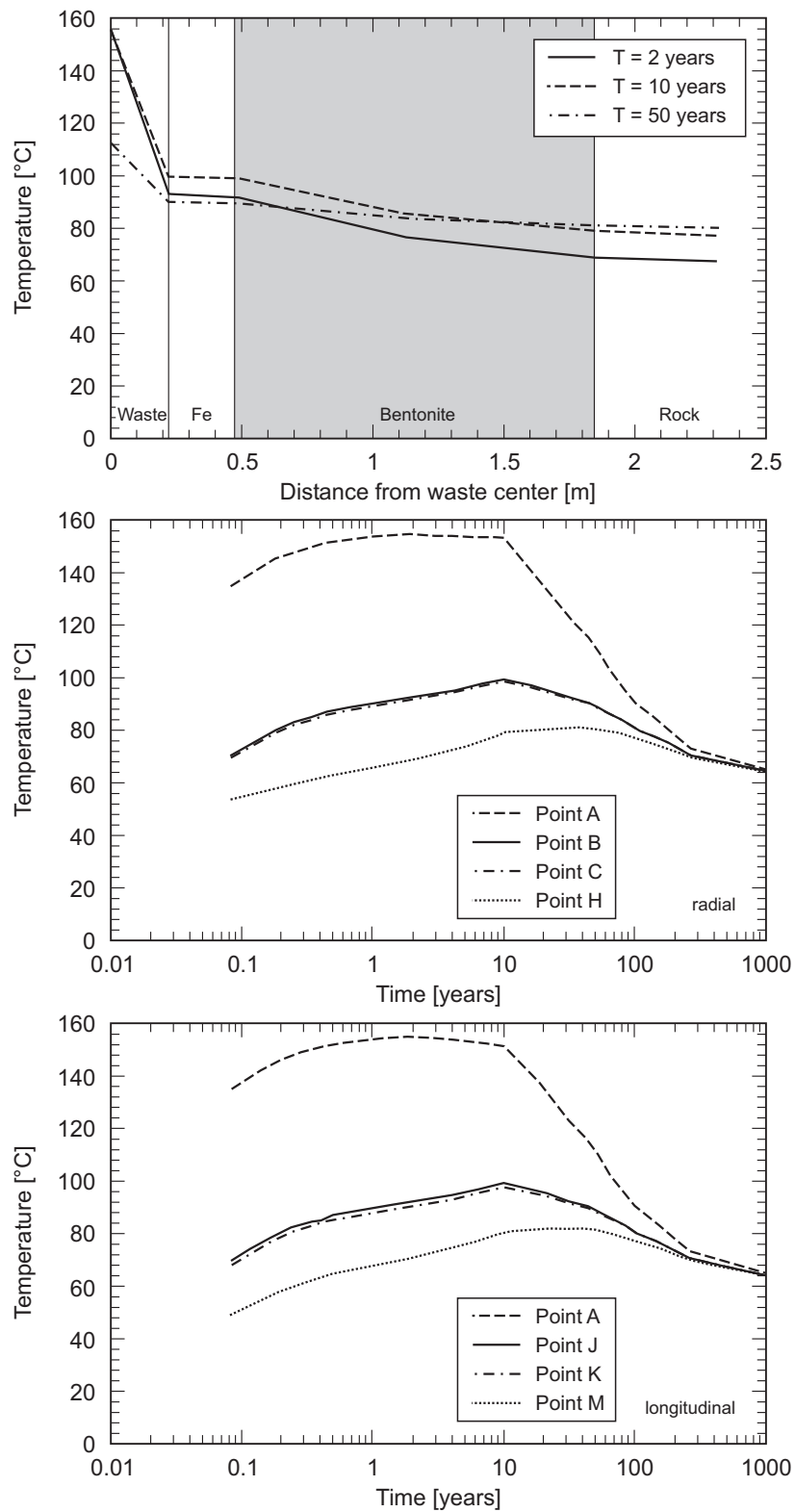


Fig. 3-14: Temperature profiles and temperature-time histories of Analysis No. 11

Top: Temperature profile in a radial direction from the center at the indicated times. Middle and bottom: Temperature-time histories in radial and longitudinal direction, respectively, at the indicated locations.

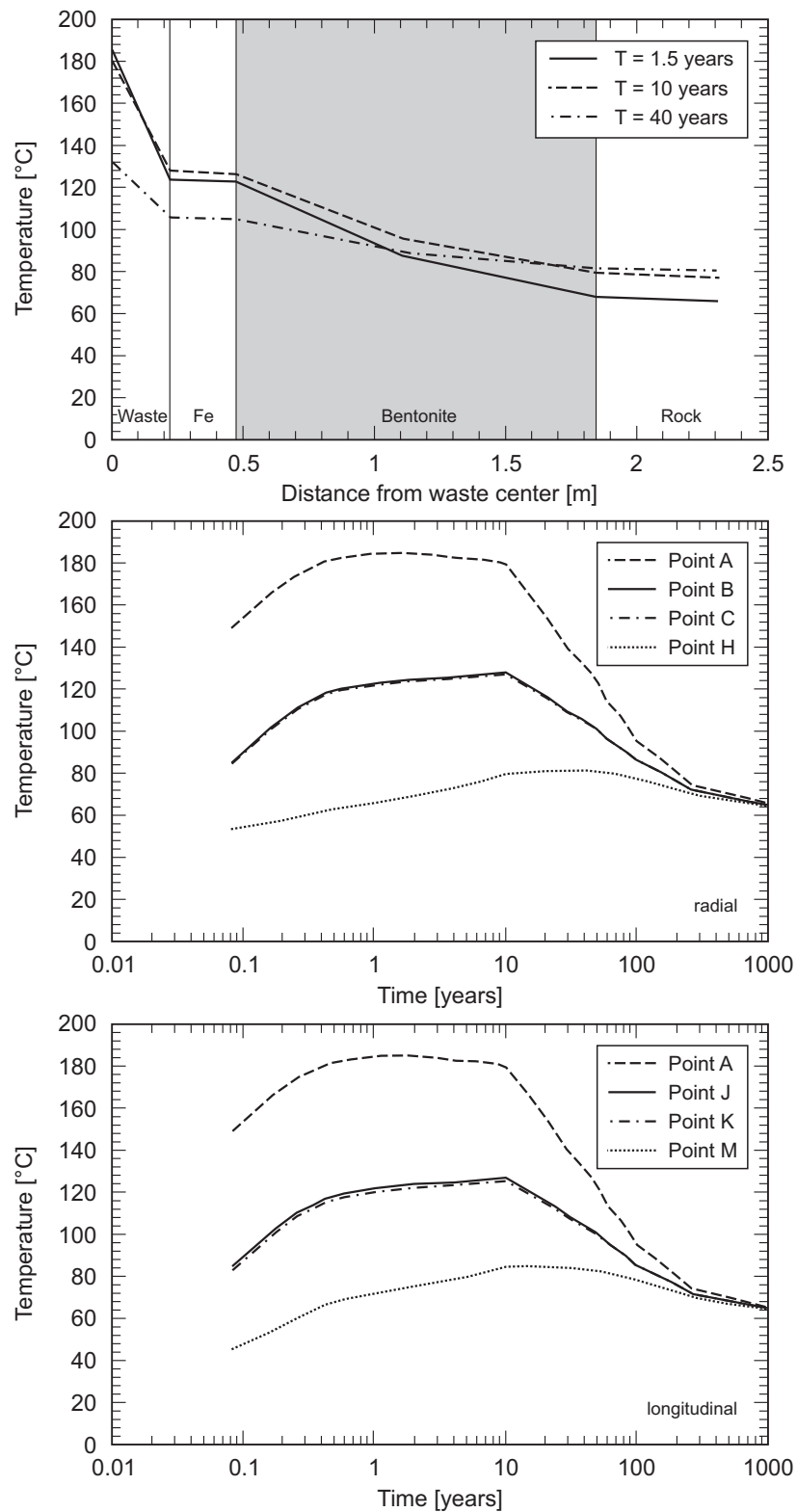


Fig. 3-15: Temperature profiles and temperature-time histories of Analysis No. 12

Top: Temperature profile in a radial direction from the center at the indicated times. Middle and bottom: Temperature-time histories in radial and longitudinal direction, respectively, at the indicated locations.

3.3 Comparison with the temperature outputs for Project Gewähr 1985

The calculated temperature profiles in the present study are compared with those in Project Gewähr 1985. Figure 3-16 shows this cross-comparison of Analysis No. 1 (three-dimensional analysis with tunnel spacing $S_h = 40$ m and three air gaps) and Analysis No. 7 ($S_h = 40$ m without air gap) with the temperature profiles for Project Gewähr 1985 (two-dimensional analysis of $S_h = 40$ m with heat-conducting and radiating air gaps).

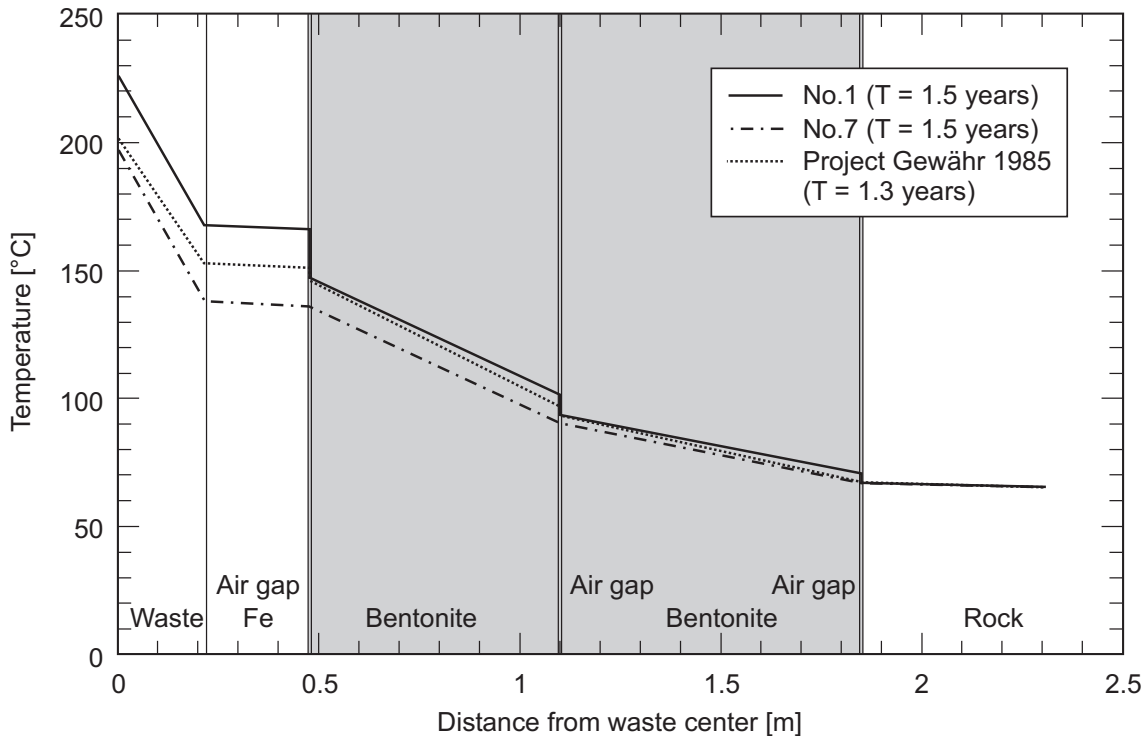


Fig. 3-16: Cross-comparison of the temperature profiles calculated in this study with those in Project Gewähr 1985

Analysis No. 1 of the present study yielded the highest temperatures in vitrified waste, canister and bentonite. In this case, air gaps are modeled as a heat-conducting material with the thermal properties of air. The second highest temperatures were obtained in Project Gewähr 1985, in which two-dimensional analyses were performed. The lowest temperatures were obtained in Analysis No. 7 of the present study, in which air gaps are not taken into account. Note that the different analyses yielded almost identical temperatures in the host rock.

3.4 Effect of tunnel spacing on temperature distributions

To understand the effect of tunnel spacing on temperature distributions, the temperature profiles and time histories of Analyses No. 1 to 3 (air gap) and Analyses No. 7 to 9 (no air gap) are compared. The top graph in Figure 3-17 shows the temperature profiles of Analyses No. 1 (tunnel spacing $S_h = 40$ m), No. 2 ($S_h = 20$ m) and No. 3 ($S_h = 10$ m) at the times of maximum bentonite temperature. The graph in the middle of Figure 3-17 shows the temperature-time histories at the canister-bentonite interface (point D indicated in Fig. 3-3) for Analyses No. 1 to 3. The bottom graph in Figure 3-17 shows the same histories at the rock surface (point H indicated in Fig. 3-3). Figure 3-18 shows the same graphs for Analyses No. 7 to 9 (no air gap).

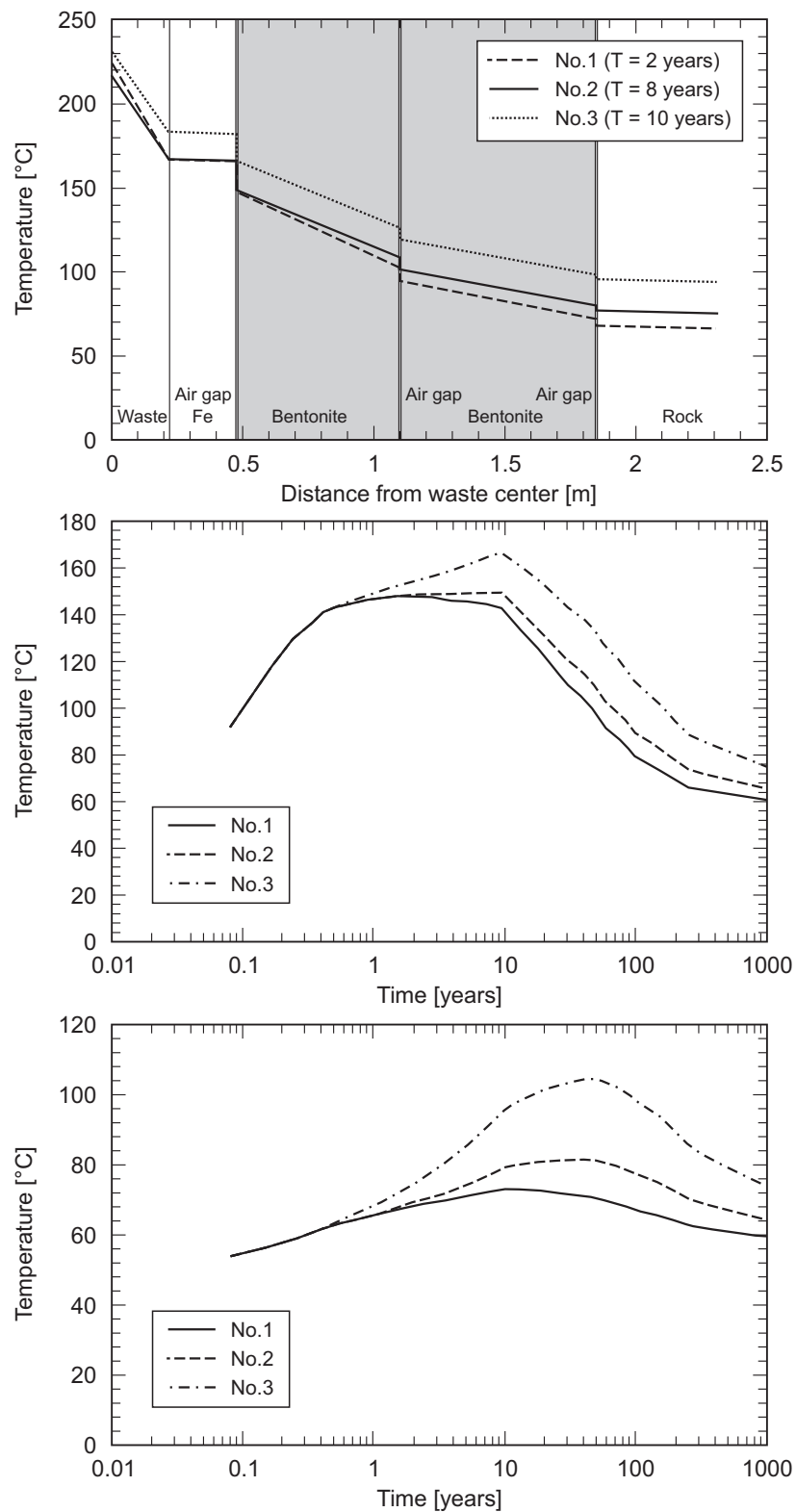


Fig. 3-17: Comparison of temperature profiles and temperature-time histories of Analyses No. 1, 2 and 3 (air gap)

Top graph: Temperature profiles at the times of maximum bentonite temperature. Middle and bottom graphs: Temperature-time histories at the canister-bentonite interface (point D) and at the rock surface (point H), respectively.

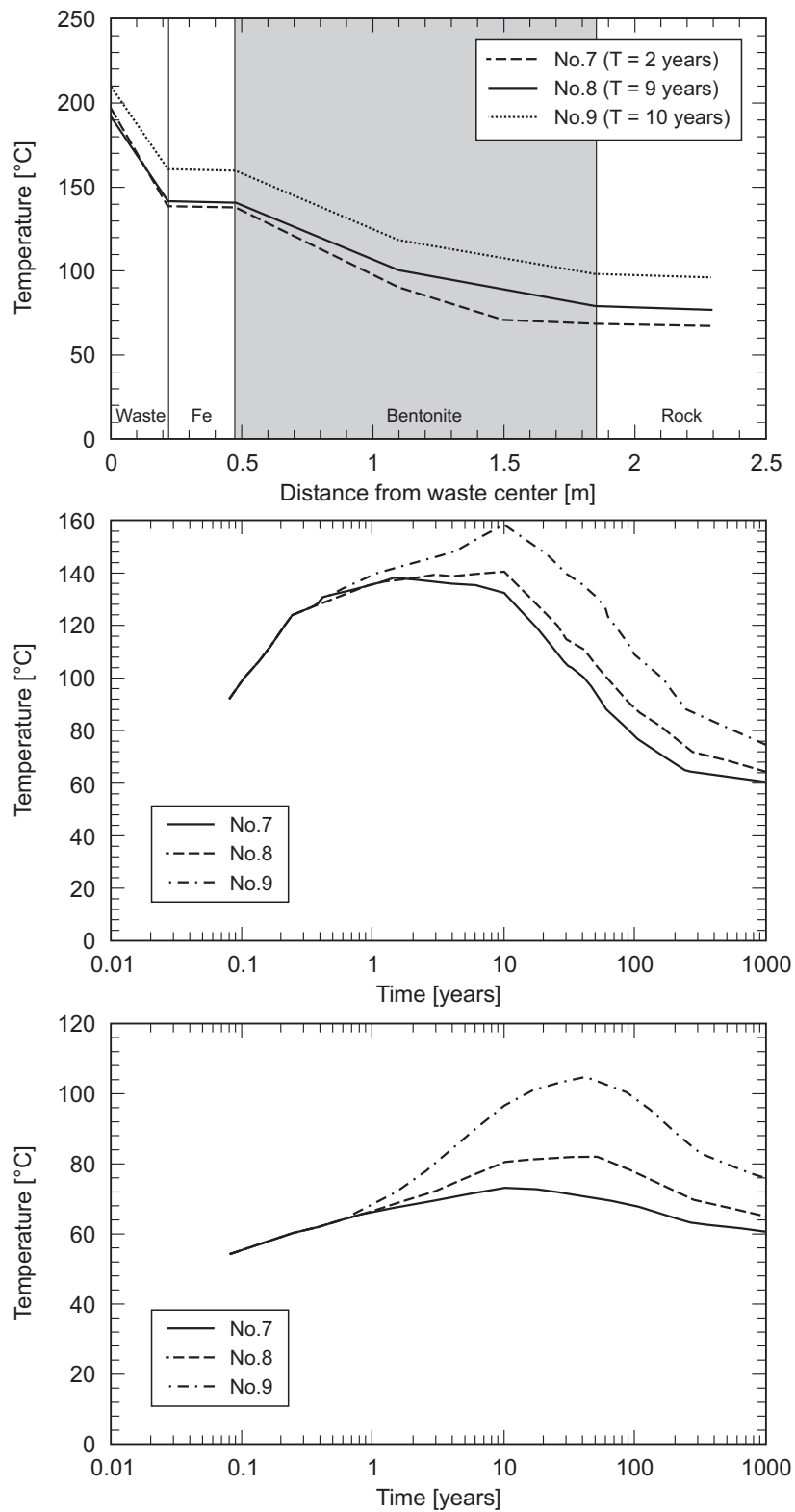


Fig. 3-18: Comparison of temperature profiles and temperature-time histories of Analyses No. 7, 8 and 9 (no air gap)

Top graph: Temperature profiles at the times of maximum bentonite temperature. Middle and bottom graphs: Temperature-time histories at the canister-bentonite interface (point D) and at the rock surface (point H), respectively.

As can be seen from these figures, there are relatively small temperature differences between Analyses No. 1 ($S_h = 40$ m) and No. 2 ($S_h = 20$ m) and between Analyses No. 7 ($S_h = 40$ m) and No. 8 ($S_h = 20$ m), but larger differences exist between Analyses No. 2 ($S_h = 20$ m) and No. 3 ($S_h = 10$ m) and between Analyses No. 8 ($S_h = 20$ m) and No. 9 ($S_h = 10$ m). As previously noted, the horizontal spacing of emplacement tunnels should therefore not be less than 20 m from the viewpoint of minimizing temperatures.

3.5 Effect of bentonite thermal properties on temperature distributions

As explained in section 2.4.1, the thermal properties of bentonite blocks depend on their water content, which is difficult to predict after emplacement in a tunnel. Thus, three approaches are chosen in this study: (A) bentonite thermal properties are assumed to vary depending on temperature (variable case $\phi = 7 - 0\%$), (B) constant water content is assumed (constant case $\phi = 2\%$) and (C) thermal properties are kept constant, with bounding parameters (bounding case).

In order to understand the effect of bentonite thermal properties on temperature distributions, the temperature profiles of Analyses No. 1 and 4, Analyses No. 2 and 5, Analyses No. 3 and 6 and Analyses No. 10 to 12 are compared in this section. Figures 3-19 to 3-22 show these comparisons of temperature profiles. From Figure 3-19, there appears to be almost no temperature difference between Analysis No. 1 ($\phi = 7 - 0\%$) and No. 4 ($\phi = 2\%$), assuming a tunnel spacing of $S_h = 40$ m in both cases. From Figure 3-20 and Figure 3-21, it can be seen that these temperature differences caused by different thermal properties of bentonite gradually become larger as tunnel spacing decreases but, even in the case of $S_h = 10$ m shown in Figure 3-21, the temperature differences are relatively small, especially in the bentonite and rock components. From these results, it can be said that the temperature distributions are not particularly sensitive to bentonite thermal properties within the parameter ranges considered.

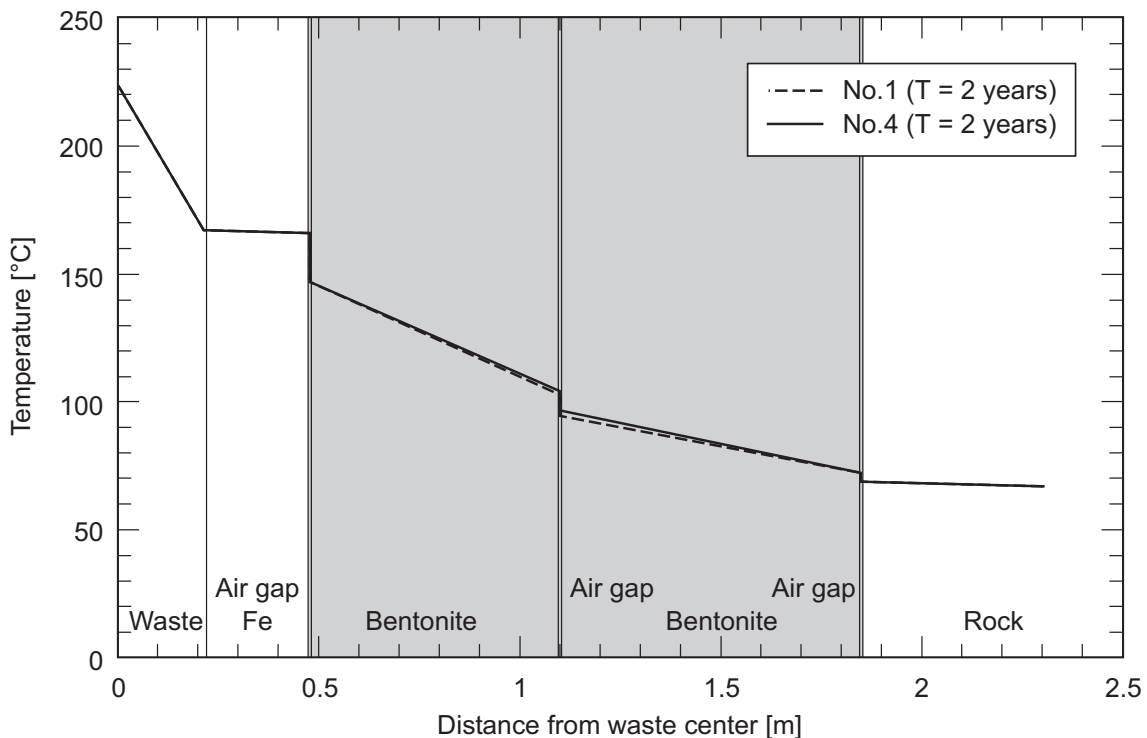


Fig. 3-19: Temperature profiles of Analyses No. 1 and 4 (tunnel spacing $S_h = 40$ m)

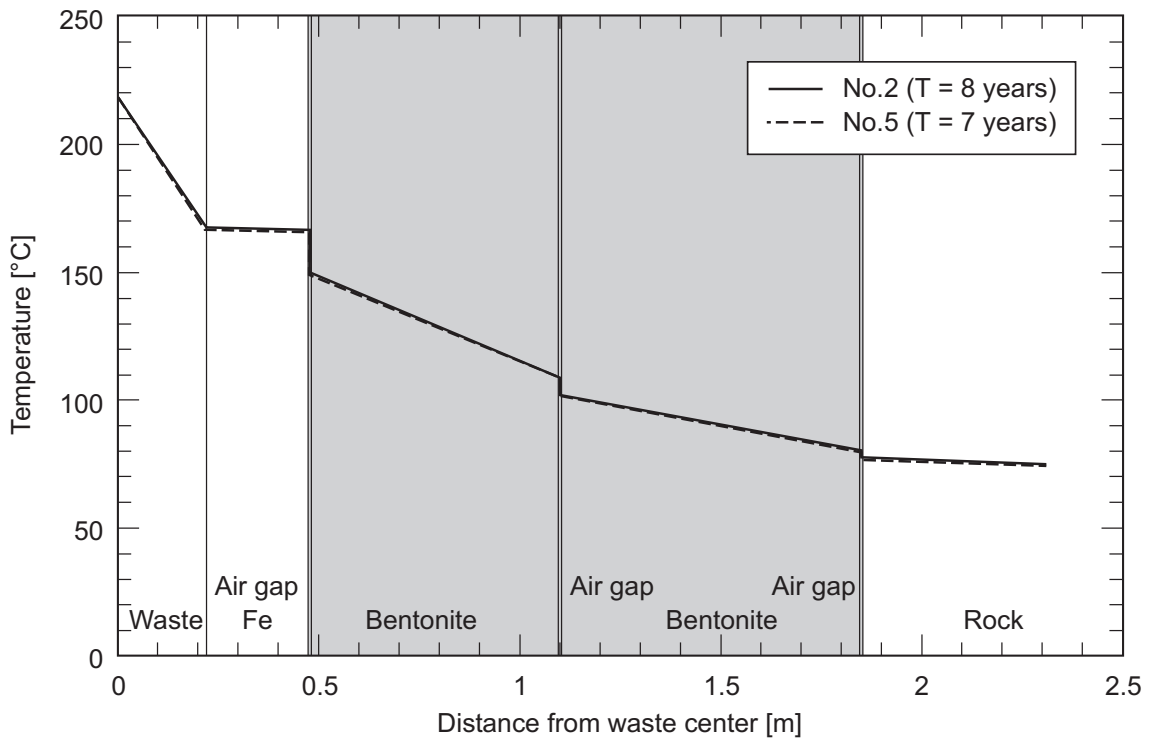


Fig. 3-20: Temperature profiles of Analyses No. 2 and 5 (tunnel spacing $S_h = 20$ m)

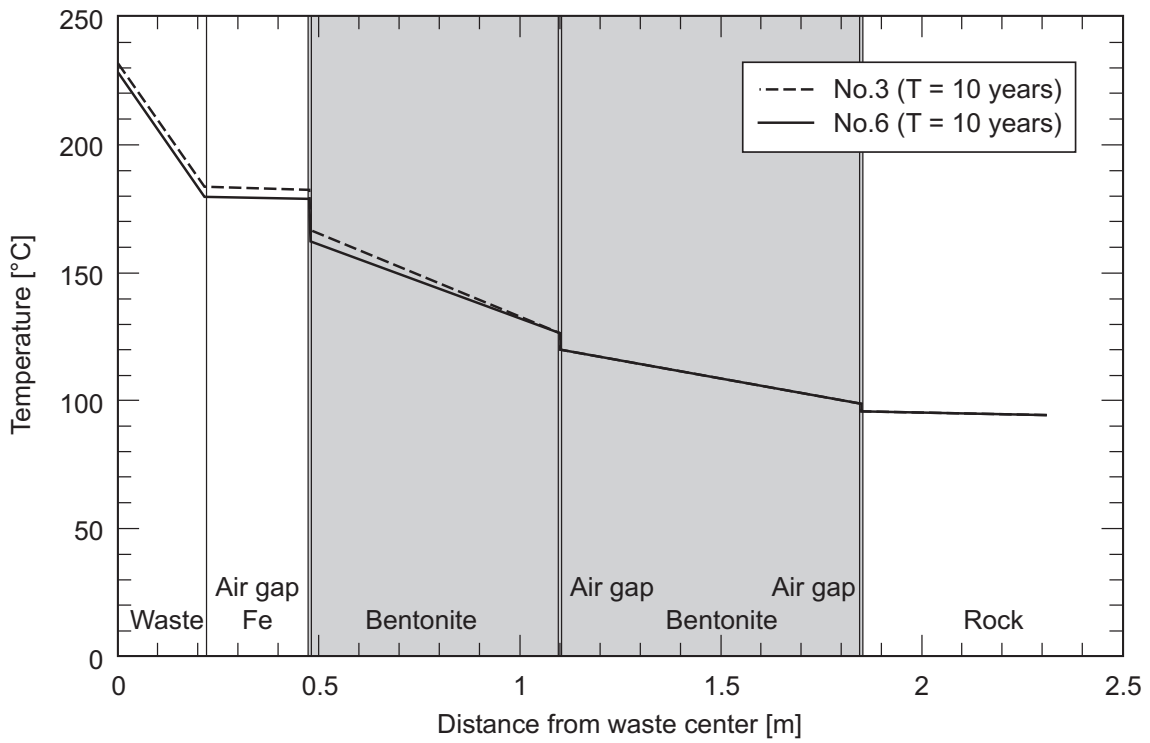


Fig. 3-21: Temperature profiles of Analyses No. 3 and 6 (tunnel spacing $S_h = 10$ m)

From Figure 3-22, Analyses No. 10 and 12 give similar temperature profiles, but there is a clear difference between Analyses No. 10 or 12 (bentonite thermal conductivity of 0.7 W/mK) and Analysis No. 11 (thermal conductivity of 1.7 W/mK). It can be concluded that the temperature distributions are sensitive to the thermal conductivity of bentonite and that they are insensitive to its heat capacity.

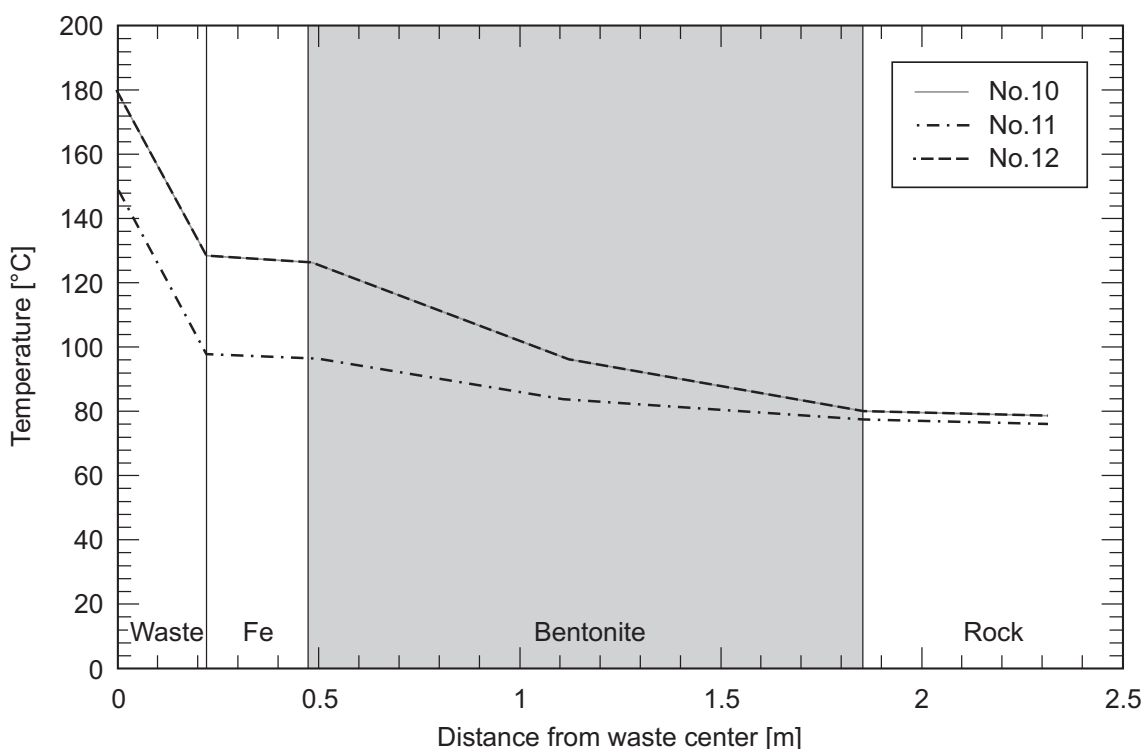


Fig. 3-22: Temperature profiles of Analyses No. 10, 11 and 12 (tunnel spacing $S_h = 20$ m)

3.6 Effect of air gaps on temperature distributions

The temperature profiles of Analyses No. 1 and 7 (tunnel spacing $S_h = 40$ m), Analyses No. 2 and 8 ($S_h = 20$ m), and Analyses No. 3 and 9 ($S_h = 10$ m) are compared to illustrate the effect of air gaps on temperature profiles. Figs. 3-23 to 3-25 show these comparisons of temperature profiles.

From these figures, it is clear that Analyses No. 1, 2 and 3 (with air gaps) give the highest temperatures. This is to be expected because air gaps act as high-performance insulators, particularly since radiative heat transfer is ignored in these calculations. Thus, these temperatures are considered to be the most conservative results. It is suggested that processes that might lead to the formation of air gaps between canister and bentonite, between bentonite blocks and between bentonite and rock should be investigated in future, because temperature distributions are sensitive to their presence.

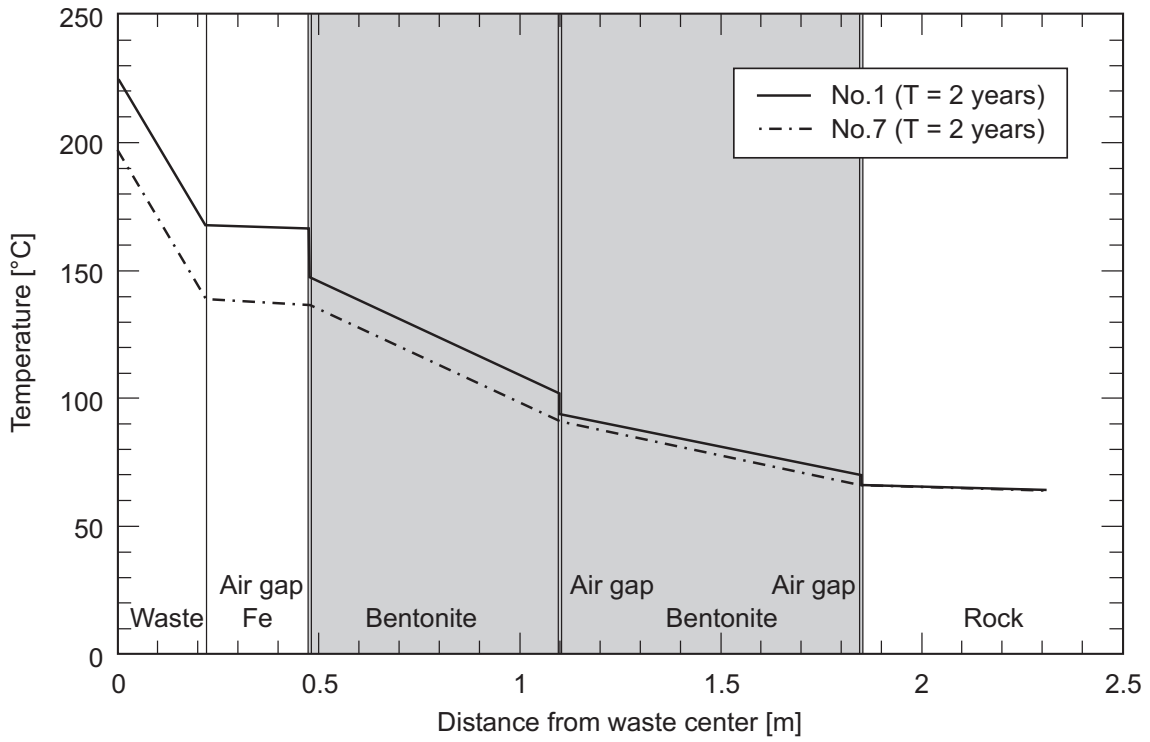


Fig. 3-23: Temperature profiles of Analyses No. 1 and 7 (tunnel spacing $S_h = 40$ m)

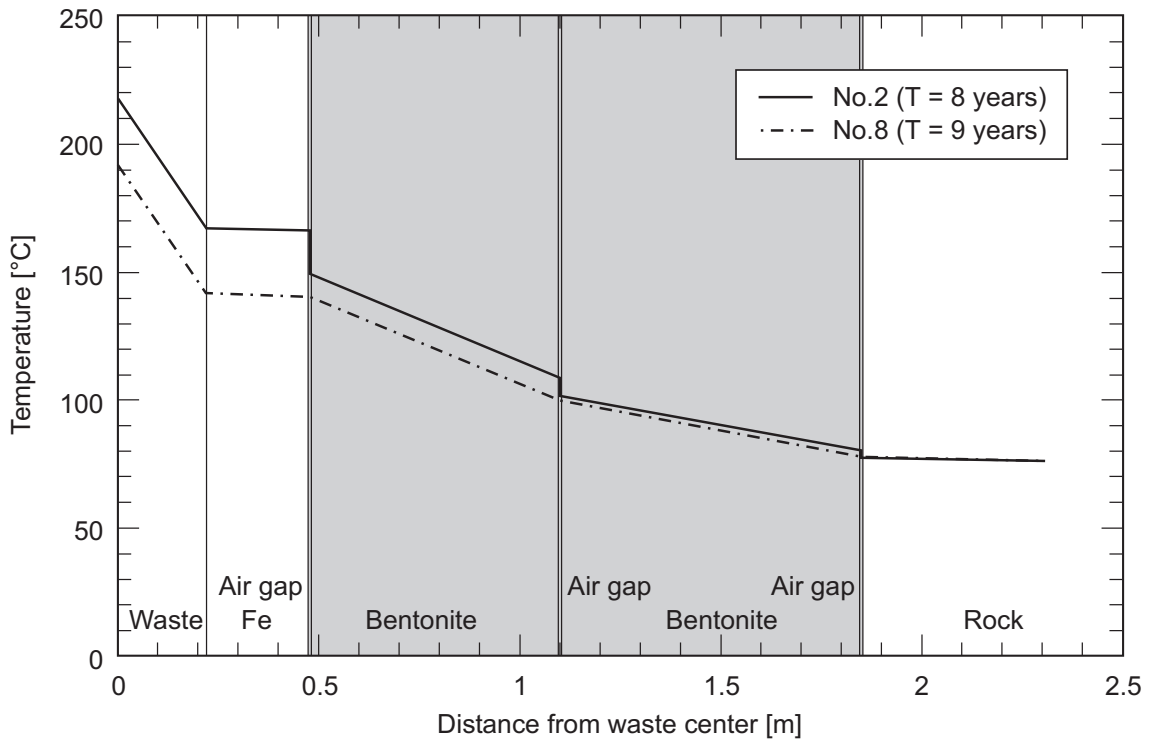


Fig. 3-24: Temperature profiles of Analyses No. 2 and 8 (tunnel spacing $S_h = 20$ m)

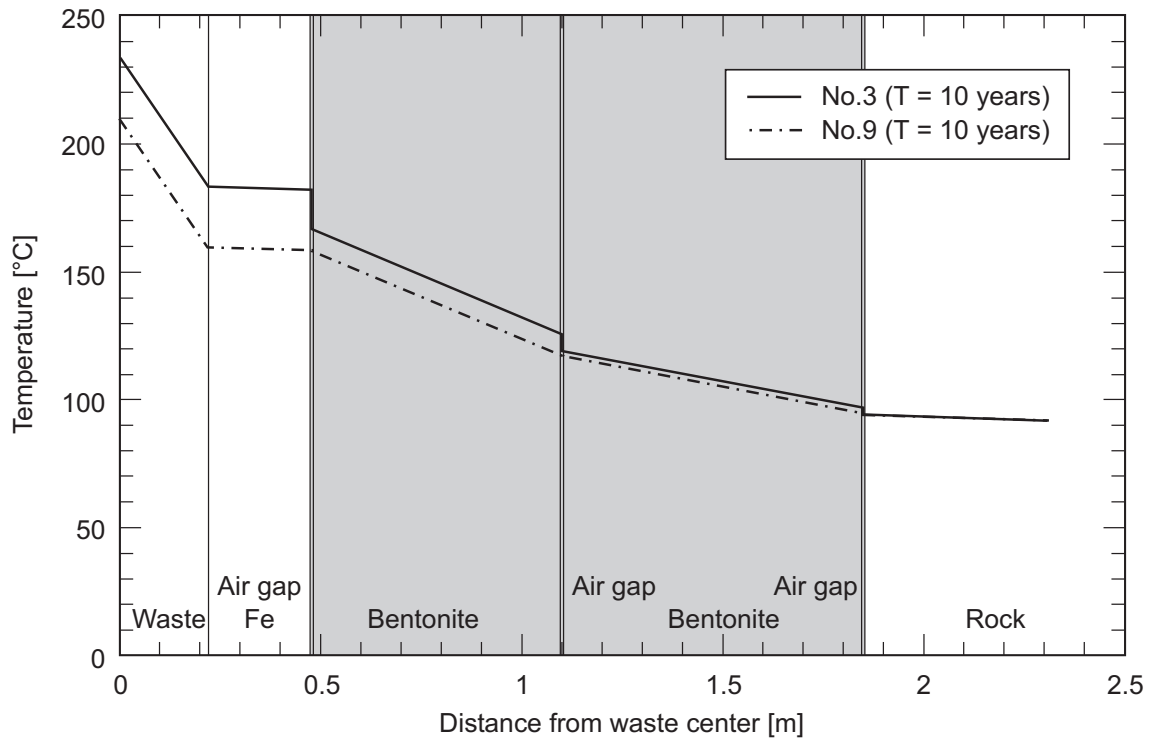


Fig. 3-25: Temperature profiles of Analyses No. 3 and 9 (tunnel spacing $S_h = 10$ m)

4 Summary and conclusions

In the Kristallin-I Project, Nagra has evaluated the disposal of vitrified HLW canisters in emplacement tunnels located at a depth of around 1200 m in the crystalline basement of Northern Switzerland (NAGRA 1994b). In support of this project, temperature distributions in the near-field arising from the radiogenic heat from the waste were analyzed numerically as a joint Nagra-Obayashi study. The main aim of the study was to understand the effect of tunnel spacing on temperature distributions in order to provide input for future optimization of emplacement tunnel layout. This report summarizes the results of temperature calculations and discusses their influence on the tunnel layout.

The numerical analyses were conducted using a three-dimensional model and the finite-element program ADINA-T. The horizontal spacing of emplacement tunnels was varied as 40 m, 20 m and 10 m. In addition, bentonite thermal properties and the presence of air gaps were also varied to investigate their influence on the results.

Most importantly, based on the maximum temperatures and temperature distributions calculated in this study, it was recommended that the horizontal spacing of emplacement tunnels should not be less than about 20 m, to ensure that thermal interactions between tunnels are negligible. The temperatures of all the components in the near-field tend to increase significantly if tunnel spacing is less than about 20 m. It should be emphasized that this conclusion is provisional, based on the idealized numerical calculations and model parameters in this study. However, the authors feel that this represents valuable information, particularly for the current phase of the HLW project in Switzerland.

Secondly, no significant temperature differences were observed between cases where the thermal properties of bentonite depend on water content ($\phi = 7 - 0\%$, Analyses No. 1 to 3) and those where its water content is kept constant ($\phi = 2\%$, Analyses No. 4 to 6). Thus, temperature distributions in the near-field were relatively insensitive to bentonite thermal properties within the range examined.

As bounding cases, Analyses No. 10 to 12 were performed with less conservative bentonite thermal conductivities (1.7 or 0.7 W/mK) and heat capacities (1.1 or 2.1 MJ/m³K), assuming that no air gaps exist and with the horizontal tunnel spacing kept at 20 m. Based on these analysis cases, temperature profiles are seen to be sensitive to the thermal conductivity of bentonite but insensitive to its thermal capacity. It is believed that realistic temperatures will lie between those of Analyses No. 10/12 and those of Analysis No. 11.

Finally, it is worth noting that the existence and duration of air gaps between a canister and bentonite blocks, between bentonite blocks and between bentonite blocks and rock is uncertain and should be investigated because temperature distributions are sensitive to the presence of such gaps.

5 References

- ALDER, J.C. & MCGINNES, D.F. (1993): Heat production values for the COGEMA vitrified residue waste (Kristallin-I project); Nagra unpublished report
- BEAR, J. (1972): Dynamics of fluids in porous media; Originally published by American Elsevier Publishing Company, Inc., Reprinted by Dover
- HOPKIRK, R.J., GILBY, D.J. & SCHWANNER, I. (1983): Preliminary calculations of the temperature distributions around a Type C (highly active) nuclear waste repository; Nagra Technical Report NTB 83-20, Nagra, Baden, Switzerland
- HOPKIRK, R.J. & WAGNER, W.H. (1986): Thermal loading in the near field of repositories for high and intermediate level nuclear waste; Nagra Technical Report NTB 85-54, Nagra, Baden, Switzerland
- HOPKIRK, R.J. & ZUIDEMA, P. (1992): Temperaturberechnungen für ein Endlager für hochaktive Abfälle in Sedimenten: Unterlagen zum Zwischenbericht der Sedimentstudie; Nagra unpublished report (in German)
- JAO (Japan Astronomical Observatory, 1991): Chronological table of science; Maruzen (in Japanese)
- KAHR, G. & MÜLLER-VONMOOS, M. (1982): Wärmeleitfähigkeit von Bentonit MX80 und von Montigel nach der Heizdrahtmethode; Nagra Technical Report NTB 82-06, Nagra, Baden, Switzerland (in German)
- NAGRA (1985a): Projekt Gewähr 1985 - Nuclear waste management in Switzerland: Feasibility studies and safety analyses; Nagra Project Report NGB 85-09, Baden, Switzerland
- NAGRA (1985b): Projekt Gewähr 1985 - Endlager für Hochaktive Abfälle: Bautechnik und Betriebsphase; Nagra Project Report NGB 85-03, Baden, Switzerland (in German)
- NAGRA (1985c): Projekt Gewähr 1985 - Endlager für Hochaktive Abfälle: Das System der Sicherheitsbarrieren; Nagra Project Report NGB 85-04, Baden, Switzerland (in German)
- NAGRA (1988): Sedimentstudie - Zwischenbericht 1988; Nagra Technical Report NTB 88-25, Baden, Switzerland (in German); Nagra Technical Report NTB 88-25E: Sediment Study – Disposal options for long-lived radioactive waste in Swiss sedimentary formations – Executive summary (in English)
- NAGRA (1994a): Kristallin-I - Safety assessment report; Nagra Technical Report NTB 93-22, Wettingen, Switzerland
- NAGRA (1994b): Kristallin-I - Conclusions from the regional investigation programme for siting a HLW repository in the crystalline basement of Northern Switzerland; Nagra Technical Report NTB 93-09, Wettingen, Switzerland
- PNC (1992): Research and development on geological disposal of high-level radioactive waste; PNC Technical Report TN 1410 93-059, Tokyo, Japan
- ROLPH, W.D. & BATHE, K.J. (1982): An efficient algorithm for analysis of nonlinear heat transfer with phase changes; International Journal for Numerical Methods in Engineering, Vol.18, pp.119-134
- THUNVIK, R. & BRAESTER, C. (1991): Heat propagation from a radioactive waste repository SKB 91 reference canister; SKB Technical Report TR 91-61, Stockholm, Sweden